

Thermodynamics Governing Binding of *Homo sapiens* Centrin - *Homo sapiens* Sfi1p₂₁ Complexes

by

Adalberto Díaz Casas

A thesis submitted in partial fulfillment of the requirements for the degree of

MASTER OF SCIENCE
in
CHEMISTRY

UNIVERSITY OF PUERTO RICO
MAYAGÜEZ CAMPUS
2012

Approved by:

Enrique Meléndez, PhD
Member, Graduate Committee

Date

Robert Ríos, PhD
Member, Graduate Committee

Date

Belinda Pastrana, PhD
President, Graduate Committee

Date

Paul Sundaram, PhD
Representative of Graduate Studies

Date

René Vieta, PhD
Chairperson of the Department

Date

ABSTRACT

Centrin is a member of the EF-hand superfamily of calcium-binding proteins and has a molecular weight of ~20 kDa. In *Homo sapiens*, four centrin isoforms have been determined: centrin 1 (*Hscen1*), which is found in male germ cells, certain neurons and ciliated cells, centrin 2 (*Hscen2*) and centrin 3 (*Hscen3*) are expressed in all somatic cells, and centrin 4 (*Hscen4*) found in neurons. We focused our research on Sfi1, a centrin binding protein of 1242 amino acids and comprising 23 tandem centrin-binding sites (CBS). Specifically, we studied a soluble Sfi1 peptide comprised of the 21st centrin binding site (*HsSfi1p₂₁*). *HsSfi1p₂₁* exhibits the hydrophobic triad (W₁L₄L₈) which is found to be essential for the interaction between centrin and its biological targets. Using isothermal titration calorimetry, the interaction between *Hscen1* and *HsSfi1p₂₁* was analyzed at 25°C, 30°C, 35°C, and 40°C. At 35°C, the complex shows the highest stability ($\Delta G = -10.2$ kcal/mol) and affinity ($K_a = 1.7 \times 10^7$ M⁻¹) with a favorable enthalpy ($\Delta H = -29.0$ kcal/mol) and unfavorable entropy ($-T\Delta S = 18.8$ kcal/mol). By a comparative thermodynamic analysis of the interaction of three human centrin isoforms (*Hscen1*, *Hscen2*, and *Hscen3*) with *HsSfi1* at 30°C, we found that *Hscen3-HsSfi1p₂₁* complex presented the highest stability and affinity interaction. From these results, we found that the stability on centrin-Sfi1p complex is dependent to the relative stability of centrin.

RESUMEN

Centrin es un miembro de la superfamilia de la mano EF de proteínas enlazantes de calcio y tiene un peso molecular de ~20 kDa. En *Homo sapiens*, se ha determinado cuatro isoformas de centrin: centrin 1 (*Hscen1*), el cual se encuentra en células germinales masculinas, algunas neuronas y células ciliadas, centrin 2 (*Hscen2*) y centrin 3 (*Hscen3*) están expresadas en todas las células somáticas, y centrin 4 (*Hscen4*) encontrada en neuronas. Nosotros enfocamos nuestra investigación en Sfi1, una proteína que enlaza a centrin de 1242 aminoácidos y que tiene 23 sitios para enlazar centrin. Específicamente, estudiamos un péptido soluble de Sfi1 compuesto del 21^{un} sitio de enlazar centrin (*HsSfi1p₂₁*). *HsSfi1p₂₁* exhibe la tríada hidrofóbica ($W_1L_4L_8$) el cual se ha encontrado que es esencial para la interacción entre centrin y sus objetivos biológicos. Utilizando calorimetría de titulación isotermal, la interacción entre *Hscen1* y *HsSfi1p₂₁* fue analizada a 25°C, 30°C, 35°C y 40°C. A 35°C, el complejo mostró la mayor estabilidad ($\Delta G = -10.2$ kcal/mol) y afinidad ($K_a = 1.7 \times 10^7 M^{-1}$) con una entalpía favorable ($\Delta H = -29.0$ kcal/mol) y una entropía no favorable ($-T\Delta S = 18.8$ kcal/mol). Por medio de un análisis comparativo de la interacción entre tres isoformas de centrin (*Hscen1*, *Hscen2*, and *Hscen3*) con *HsSfi1p₂₁* a 30°C, encontramos que el complejo *Hscen3-HsSfi1p₂₁* presentó la interacción con mayor estabilidad y afinidad. Con estos resultados, se encontró que la estabilidad del complejo centrin-Sfi1p es dependiente de la estabilidad relativa de centrin.

DEDICATION

First, I want to dedicate this thesis to **God** because He chose me in Him before the foundation of the world to be holy and without blemish before Him in love, predestinating me unto sonship through Jesus Christ to Himself, according to the good pleasure of His will (Ephesians 1:5-6, Holy Bible).

Also, this thesis is dedicated to my mother, **Leila Margarita**, my sister, **Jomary**, and my brother-in-law, **Eric**, for loving me, supporting me and motivating me in an unconditional way.

Finally, this thesis is dedicated to **my brothers and sisters in Christ**, my spiritual family, for their prayers, their care, shepherding and fellowship through all these years.

AKNOWLEDGMENT

I want to thank God because in His sovereignty, He led me to study at this time and to strengthen me throughout this path. A special thanks to Dr. Belinda Pastrana, the Chair of my committee, for giving me the opportunity to be part of her research group and carry out my Master's degree research thesis under her supervision and guidance. I appreciate very much her love for her research project and the knowledge that I received from her through these years. I also thank my graduate committee, Dr. Enrique Meléndez and Dr. Robert Ríos, for their support and recommendations. To Dr. Pastrana's research group, especially Daniel Narvaéz, Ana María Gómez, Marie Cely Rosado, Ruth Almodovar, and Aslin Rodríguez for all the help and support I received from them through these years. I thank Lizbeth Irizarry, Ana María Ortiz, Melissa Castillo, and Brenda Ortiz for their collaboration in the expression and purification of centrins. A special thanks to Tatiana Garcés for her friendship, help and collaboration in the crystallization assay presented in this thesis. I also thank Dr. Jorge Ríos for his help, recommendations, and support in the crystallization assay mentioned above. I want to thank Dr. Juan López and his research group, for giving us the opportunity to use the digital microscope. I thank the Department of Chemistry for accepting me as a graduate student and providing me financial support.

I thank my mother, Leila Margarita, for her love, tender care and support. Also I thank my sister Jomary and my brother-in-law Eric for love and support. I thank God for blessing me with the family that has giving me. Finally, I want to thank the brother and sisters from the church in Humacao and Mayagüez for their prayers, shepherding, and fellowship. All these things become a spiritual supply that has strengthened me through these years.

TABLE OF CONTENTS

Table of Contents.....	vii
List of Tables	ix
List of Figures and Schemes	x
CHAPTER I: JUSTIFICATION	1
Objectives	4
Hypothesis	4
CHAPTER II: PREVIOUS WORK.....	5
Centrin, a member of the EF-hand superfamily of calcium binding proteins	5
• <i>Centrin structure</i>	11
Studies of Centrin-biological Target Complexes	17
• <i>Centrin-Mellitin complex</i>	17
• <i>Centrin-XPC complex</i>	22
• <i>Centrin-Kar1 complex</i>	27
• <i>Sac3-Cdc31-Sus1 ternary complex</i>	30
Sfi1, a centrin binding protein first identified in yeast	34
Isothermal titration calorimetry	40
CHAPTER III: MATERIALS AND METHODS	46
<i>Protein and peptide preparation</i>	46
<i>Isothermal titration calorimetry</i>	47
<i>Analysis of ITC Data</i>	47
Crystallization Assay	48
CHAPTER IV: RESULTS AND DISCUSSION	52
Analysis of <i>HsSfi1</i> _{p21}	52
• <i>Mass Spectrometry and High Performance Liquid</i> <i>Chromatography</i>	52

- *HsSfi1p₂₁ sequence analysis*..... 54
- *Thermodynamic analyses and crystallization of the interaction between Hscen1 and HsSfi1p₂₁* 58
- *A comparative analysis of the interaction between human centrin isoforms and HsSfi1p₂₁* 69

CHAPTER V: CONCLUSIONS..... 75

CHAPTER VI: FUTURE WORK 77

REFERENCES 78

APPENDIX A 88

APPENDIX B 89

APPENDIX C 90

LIST OF TABLES

Table 1. QIAGEN® EasyXtal pre-screen suite composition table	49
Table 2. Pre-screen assay suite composition tables.....	51
Table 3. Summary of the thermodynamic data of the interaction between <i>Hscen1</i> (WT) and <i>HsSfi1p₂₁</i>	64
Table 4. Summary of the thermodynamic data for the interaction between <i>Homo sapiens</i> centrin isoforms with <i>HsSfi1p₂₁</i> at 30 °C.....	73

LIST OF FIGURES AND SCHEMES

Figure 1. Transfection of HeLa cells with GFP- <i>HsSfi1</i>	2
Figure 2. Localization of Cdc31 at the half bridge of the spindle pole body	7
Scheme 1. Analysis of centrins amino acids sequence	10
Figure 3. Ribbon structure of <i>Hscen2</i>	13
Scheme 2. The EF-hand loop motif in centrins.....	14
Figure 4. The EF-hand motif and calcium coordination	15
Figure 5. Ribbon structure of <i>Crcen</i> -MLT complex	19
Figure 6. A comparative thermodynamic analysis of CaBP-MLT complexes.....	21
Figure 7. Ribbon structure of <i>Hscen2</i> -XPC complex	24
Figure 8. Sequence alignment of the centrin binding sites within XPC in five organism	25
Figure 9. Helical wheel plot of the centrin binding site of XPC	26
Figure 10. Ribbon structure of C- <i>Crcen</i> -Kar1p complex.....	28
Figure 11. Key interactions stabilizing the complex of C- <i>Crcen</i> with Kar1p	29
Figure 12. Ribbon structure of Sac3-Cdc31-Sus1 ternary complex.....	31
Figure 13. Analysis of the interaction between Cdc31 with Sac3p	33
Figure 14. Duplication of the yeast spindle pole body is regulated by Sfi1/centrin.....	37
Figure 15. Ribbon structure of Cdc31-ScSfi1 complex	38

Figure 16. Sequence logos of Sfi1 repeats in <i>S. cerevisiae</i> and potential homologues in <i>S. pombe</i> (<i>SpSfi1</i>), <i>H. sapiens</i> (<i>HsSfi1</i>)	39
Figure 17. Diagram of ITC cell and syringe.....	43
Figure 18. Representation of ITC data.....	44
Figure 19. Illustration of the binding energy involved in an interaction between a small molecules and its target	45
Figure 20. Mass Spectrometry and HPLC results from <i>HsSfi1p₂₁</i>	53
Figure 21. Sequence analysis of <i>HsSfi1p₂₁</i>	56
Figure 22. Helical wheel plot of the N-terminal and C-terminal ends of <i>HsSfi1p₂₁</i>	57
Figure 23. ITC isotherms of the interaction between <i>Hscen1</i> (WT) with <i>HsSfi1p₂₁</i> at 25°C	60
Figure 24. ITC isotherms of the interaction between <i>Hscen1</i> (WT) with <i>HsSfi1p₂₁</i> at 30°C	61
Figure 25. ITC isotherms of the interaction between <i>Hscen1</i> (WT) with <i>HsSfi1p₂₁</i> at 35°C	62
Figure 26. ITC isotherms of the interaction between <i>Hscen1</i> (WT) with <i>HsSfi1p₂₁</i> at 40°C	63
Figure 27. Determination of the change in heat capacity by the graph of ΔH as a function of temperature	65
Figure 28. Optimization micro crystals of <i>Hscen1-HsSfi1p₂₁</i> complex.....	66
Figure 29. Optimization of needle crystals of <i>Hscen1-HsSfi1p₂₁</i> complex.....	67

Figure 30. Optimization of crystals of <i>Hscen1-HsSfi1p₂₁</i> complex	68
Figure 31. ITC isotherms of the interaction between <i>Hscen2</i> (WT) with <i>HsSfi1p₂₁</i> at 30°C	71
Figure 32. ITC isotherms of the interaction between <i>Hscen3</i> (WT) with <i>HsSfi1p₂₁</i> at 30°C	72
Figure 33. A comparative thermodynamic analysis of the interactions of <i>Homo sapiens</i> centrins and <i>HsSfi1p₂₁</i>	74

CHAPTER I

JUSTIFICATION

The study of centrin and its biological targets can be used to determine one of the proteins biological functions. Centrin has many biological targets, which in the case of this research were focused on Sfi1 first identified in yeast. Sfi1 is a 1242 amino acid protein comprised of 23 tandem centrin binding sites (CBS), including the consensus pattern $AX_7LLX_3F/LX_2WK/R$ where the X represents any residue [1, 2]. This centrin binding protein is mainly localized in the centrioles of higher eukaryotes [1]. More importantly, Sfi1 was determined to be co-localized with centrin in the centrioles (Figure 1). Early studies suggest that in order for centrin to carry out its role in spindle pole body (SPB) duplication in yeast and centriole duplication in mammals, this protein needs to interact with other biological targets, one of which is Sfi1 [1, 3]. The centrin-Sfi1p complex has previously been studied using other Sfi1's centrin binding sites [4, 5]. These studies have shown that the binding affinity between centrin and Sfi1 is moderately dependent on Ca^{+2} concentrations [4, 5].

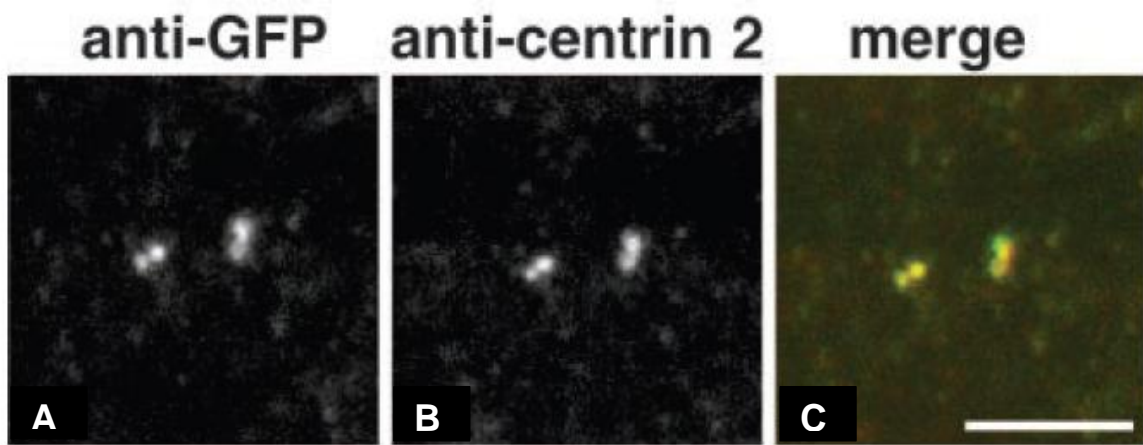


Figure 1. Transfection of HeLa cells with GFP-*HsSfi1*. Staining of the centrosome region with anti-GFP-*HsSfi1* (A), anti-centrin 2 (B), and corresponding merged images (C) (*Adapted from Kilmartin 2003 [1]*).

Isothermal titration calorimetry (ITC) is a powerful technique that directly measures the energy associated with the interaction between a protein or peptide and a target molecule. We are interested in studying protein-target peptide interactions. An ITC experiment is carried out by the addition of one of the proteins into the reaction cell containing the biological target. Also, the analysis of the data yields the stoichiometry (n), its affinity constant (K_a), the change in enthalpy of binding (ΔH_B), the change in entropy of binding (ΔS_B), and the change in Gibbs free energy (ΔG_B) of binding [6]. These parameters help us to define the affinity and stability of the complex. Also, through further analysis we can determine if a conformational change occurs during complex formation.

In this research, we study specifically the interaction of *Homo sapiens* centrin with a soluble Sfi1 peptide comprised of the 21st centrin binding site (*HsSfi1p₂₁*) using isothermal titration calorimetry (ITC). The results presented herein are novel in that they are a comparative study of the energetics of the binding process between full length centrins, specifically: *Hscen1*, *Hscen2*, and *Hscen3* with *HsSfi1p*. These studies will aid in further understanding the interaction between centrin and Sfi1p and establish their relative stability as complexes. The information provided may lead to drug design of inhibitors of the centrin-Sfi1p₂₁ complex. Thus, our interest in performing the proposed thermodynamics studies of centrin-Sfi1p₂₁ complexes.

OBJECTIVES

The following are the proposed objectives concerning this study:

- To determine the thermodynamics governing the binding of the centrin-Sfi1 complex.
- To determine the relative stability of the centrin-Sfi1 complex.
- To determine the relative affinity of the centrin-Sfi1 complex.

HYPOTHESIS

In this thesis, we propose the following working hypothesis. First, because the binding affinity between centrin and Sfi1p is moderately dependent on Ca^{+2} concentrations [4] and each EF-hand motif within centrin binds Ca^{+2} with different affinities, each centrin isoform can bind to Sfi1p with a different affinity. Also, because centrin may bind its biological targets constitutively through a hydrophobic surface [7-9] of the C-terminal domain, the affinity centrin exhibits for its biological target peptide is affected by key hydrophobic residues spatially located within the binding interface. Finally, we propose that the stability of the centrin-Sfi1p complex is dependent on the relative stability of centrin.

CHAPTER II

PREVIOUS WORK

Centrin, a member of the EF-hand superfamily of calcium binding proteins

Centrin is a calcium binding protein (CaBP) comprised of ~170 amino acids and a molecular weight of ~20 kDa. This protein was discovered in 1984 by Dr. Jeffrey L. Salisbury in the flagellar apparatus of *Tetraselmis striata* where it is directly responsible for the contraction of calcium-sensitive structures [10]. Centrin is closely related to the ubiquitous calcium sensor calmodulin (CaM) and these calcium binding proteins share approximately 50% sequence identity. Hartman and Fedorov show that centrin is one of 350 “eukaryotic signature proteins” (ESPs), therefore this protein is found in eukaryotic cells but have no significant homology to proteins in archaea and bacteria. Thus, this protein is considered critical for the structure and function of the eukaryotic cell [3, 11]. Centrins were shown to be associated with the microtubule organizing center (MTOC) [12, 13]. Also, in yeast *Saccharomyces cerevisiae* Cdc31, a centrin homolog, is crucial in the cell cycle via its regulation of the duplication of the spindle pole body (SPB), which is critical to the MTOC shown in Figure 2 [14, 15]. The interaction between Cdc31 and Kar1 is required during the first stage of SPB. Also, Cdc31 recruits Msp3 at the half bridge of SPB. Furthermore, Cdc31

specifically interacts with other proteins, like Kic1, whose activity may regulate SPB duplication [14]. Figure 2 show the localization of Cdc31 at the half bridge of SPB.

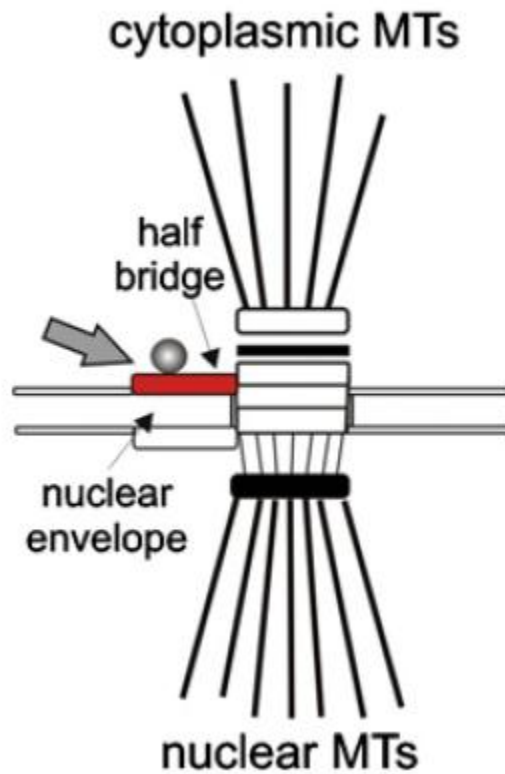


Figure 2. Localization of Cdc31 at the half bridge of the spindle pole body. The localization of Cdc31 is indicated in red and by an arrow (*Adapted from Trojan et al. 2008 [14]*).

In green algae, *Chlamydomonas reinhardtii* centrin (*Crcen*) plays an essential role in a cell-cycle-dependent duplication and separation of the MTOC [16]. Thus, *Crcen* is associated with the initiation of flagellar excision during the microtubule severing [17].

In higher eukaryotes, such as *Mus musculus* and *Homo sapiens*, there are four centrin isoforms which are centrin 1, centrin 2, centrin 3, and centrin 4 [3, 18]. In *Homo sapiens*, centrin 1 (*Hscen1*) and centrin 2 (*Hscen2*) have a sequence identity of approximately 84%, but only 53% identity with centrin 3 (*Hscen3*) (Scheme 1). Conversely, *Hscen1* and *Hscen2* are more closely related to *Crcen* than *Hscen3* [19]. The N-terminal domain, specially the first 20 amino acids shows the most variable region of the centrin sequences [3, 20]. In addition to the EF-hand motifs, the C-terminal half presents the most conserved region, particularly the short sequence -KKTSLY which has been identified as a phosphorylation consensus sequence for various kinases [3, 16]. This sequence is missing in *Hscen3* [3] (Scheme 1). Centrin 1 is an isoform that is restricted to the male germ cell, neurons and highly ciliated cells [3, 18, 20]. This isoform is localized at the base of the flagella within the sperm. During the first zygote division the sperm contributes the mother centriole to the ovum [21]. Recent clinical studies show that abnormalities in centrin 1 may be related to male infertility [22-24]. Contrary to centrin 1, centrin 2 and centrin 3 are ubiquitously expressed in all somatic cells. Centrin 2 is required for centriole separation and duplication, a key

event in cell division [25, 26]. Also, centrin 2 along with xeroderma pigmentosum group C (XPC) and small ubiquitin-like modifier (SUMO 2/3) regulates nucleotide excision repair (NER) in the nucleus [27-29]. Moreover, Resendes et al. in 2008 [30] showed that centrin 2 localizes to the nuclear pore and plays a functional role in mRNA export. Centrin 3, a centrin gene closely related to Cdc31 (Scheme 1), is involved in the duplication of the spindle poles in HeLa cells [19, 31]. *Homo sapiens* centrin 4 (*Hscen4*), a pseudogene, is found in neuronal cells within the brain [32]. The four isoforms of centrin are localized in the connecting cilium within the apparatus of the photoreceptor cells [16].

Centrin structure

The most characteristic domains of centrin are the four helix-loop-helix EF-hand consensus motif (Figure 3). It is within the loop region that the residues that bind calcium are located and are described in a Cartesian coordinate system (X, Y, Z, -X, -Y, -Z) [33]. Because Ca^{+2} is a “hard acid” metal ion, it likes to coordinate with “hard base” ligands. This provides an interaction dominated by ionic forces. Thus, the oxygen is the coordinating atom of choice. It is for this reason that we can observe in the ‘loop’ part of the EF-hand a region rich in aspartates and glutamates which are negatively charged amino acids. The residues that coordinate with calcium are in the positions 1(X), 3(Y), 5(Z), 7(-Y), 9(-X), and 12(-Z) (Scheme 2). The X, Y, Z, and -Z positions coordinate calcium through the aspartate and glutamate carboxylate. The -Y position coordinates calcium via the backbone carbonyl group, while the residues in the -X position coordinates indirectly with calcium through a water molecule. As we can see in Figure 4, the geometry adopted between the Ca^{+2} and its ligands is pentagonal bipyramid [34-35]. These calcium binding sites define centrin as a member of the EF-hand superfamily of calcium binding proteins. A tethered helix is found between the second and third EF-hand motifs, thus generating a dumbbell arrangement with two independent domains. Trojan and his colleagues in 2008 [16] showed that although the four EF-hand motifs of centrin are highly conserved, each EF-hand motifs binds Ca^{+2} with different affinities. Centrin undergoes conformational

changes from a close to an open domain upon binding Ca^{+2} ions [33, 36]. In the Ca^{+2} -bound state (holo form), the hydrophobic amino acids that were buried in the apo form (without the Ca^{+2} ion) are now exposed to the solvent. Thus, the Ca^{+2} binding represent the most important, but not the only, molecular regulatory mechanism of centrin [16].

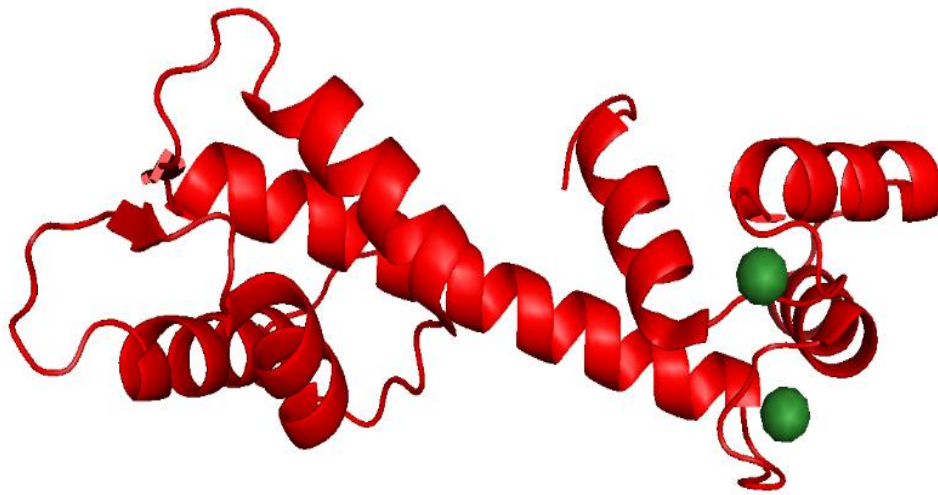


Figure 3. Ribbon structure of *Hscen2* (red) (PDB ID 2GGM). In this model representative of full length centrin comprised of four EF-hands. Two calcium ions (green spheres) are bind in helix-loop-helix motifs located in the C-terminal end of centrin 2 (*Adapted from Thompson et al. 2006 [45]*).

EF-hand 1												
	X		Y		Z		-Y		-X			-Z
Hscen1	D	V	D	G	S	G	T	I	D	A	K	E
Hscen2	D	A	D	G	T	G	T	I	D	V	K	E
Hscen3	D	T	D	K	D	E	A	I	D	Y	H	E
Mmcen4	D	I	D	G	S	G	T	I	D	L	K	E
Crcen	D	T	D	G	S	G	T	I	D	A	K	E
Cdc31	D	M	N	N	D	G	F	L	D	Y	H	E
HsCaM	D	K	D	G	D	G	T	I	T	T	K	E

EF-hand 2												
	X		Y		Z		-Y		-X			-Z
Hscen1	D	R	E	G	T	G	K	I	S	F	N	D
Hscen2	D	K	E	G	T	G	K	M	N	F	G	D
Hscen3	D	R	E	A	T	G	K	I	T	F	E	D
Mmcen4	D	K	E	G	T	G	T	I	C	F	E	D
Crcen	D	K	D	G	S	G	T	I	D	F	E	E
Cdc31	D	S	E	G	R	H	L	M	K	Y	D	D
HsCaM	D	A	D	G	N	G	T	I	D	F	P	E

EF-hand 3												
	X		Y		Z		-Y		-X			-Z
Hscen1	D	D	D	E	T	G	K	I	S	F	K	N
Hscen2	D	D	D	E	T	G	K	I	S	F	K	N
Hscen3	D	D	D	D	S	G	K	I	S	L	R	N
Mmcen4	D	D	D	A	T	G	S	I	S	L	N	N
Crcen	D	D	D	N	S	G	T	I	T	I	K	D
Cdc31	D	D	D	H	T	G	K	I	S	I	K	N
HsCaM	D	K	D	G	N	G	Y	I	S	A	A	E

EF-hand 4												
	X		Y		Z		-Y		-X			-Z
Hscen1	D	R	D	G	D	G	E	V	N	E	E	E
Hscen2	D	R	D	G	D	G	E	V	S	E	Q	E
Hscen3	D	K	D	G	D	G	E	I	N	Q	E	E
Mmcen4	D	R	D	G	D	G	E	I	N	E	E	E
Crcen	D	R	N	D	D	N	E	I	D	E	D	E
Cdc31	D	L	D	G	D	G	E	I	N	E	N	E
HsCaM	D	I	D	G	D	G	Q	V	N	Y	E	E

Scheme 2. The EF-hand loop motifs in centrins and calmodulin. The four EF-hand loop motif in *Homo sapiens* centrins (*Hscen1*, *Hscen2*, and *Hscen3*), *Mus musculus* centrin 4 (*Mmcen4*), *Chlamydomonas reinhartii* centrin (*Crcen*), *Saccharomyces cerevisiae* centrin homolog (*Cdc31*), and *Homo sapiens* calmodulin (*HsCaM*).

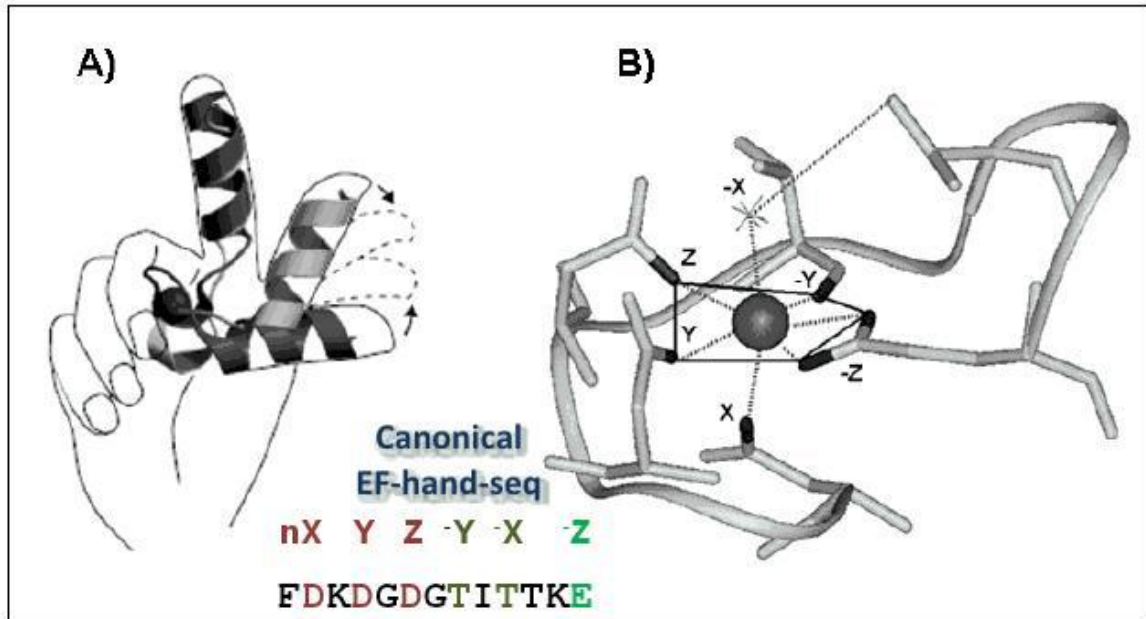


Figure 4. The EF-hand motif and calcium coordination (A) The EF-hand motif. (B) Calcium coordination. At position X and Y, the side chains of Asp or Asn are usually found; the side chains of Asp, Asn or Ser are found in Z and a backbone peptide carbonyl oxygen lies at -Y. -X commonly is a water molecule and -Z is a conserved bidentate ligand, Asp⁻ or Glu⁻ (*Adapted from Lewit-Bentley and Réty 2000 [34], Kretsinger, et. al., 1973 [35]*).

The C-terminal domain of *Crcen* plays a regulatory role that is dependent on the Ca^{+2} binding state [7, 36, 37]. The N-terminal imparts stability and directs localization [37, 38]. Chazin's group in 2006 [38] stated that the N-terminal domain of *Crcen* may serve as a calcium sensor. *Crcen* binds Ca^{+2} ions with a dissociation constant ranging from 1 nM to 0.1 mM [3].

Studies of Centrin-biological Target Complexes

Centrin-Melittin complex

Melittin (MLT) is a peptide from bee venom composed of 26 amino acids (GIGAILKVLATGLPTLISWIKNKRKQ). This peptide was used as a model to study the interactions between calcium binding proteins and peptides [8, 39-43]. Observing its amino acids sequence, we can note that MLT is an amphipathic peptide because the first 20 amino acid are primarily hydrophobic residues whereas the C-terminal end has many positively charged residues. Cox and his co-workers in 2000 [8] reported for *Hscen2*-MLT complex (1:1 mole ratio) that the interaction between *Hscen2* and MLT exhibits a dissociation constant (K_d) of 100 nM, whereas the estimation of the K_d of the complex between *Hscen3* fragment (residues E₂₁ through D₁₁₂) and MLT is about 20-50 nM, i.e., a 2-3 fold higher affinity than that of *Hscen2*-MLT complex [44].

Many scientists have attempted to obtain a MLT-CaBP complex structure for the past 30 years. Pastrana's group has recently published the first of such structures involving full-length *Crcen* and MLT [37]. The structure of *Crcen*-MLT complex is presented in Figure 5. This crystal structure (PDB ID 3QRX) shows that MLT interacts with the C-terminal domain of *Crcen*. The binding orientation of MLT differs from the binding orientation of XPC shown in the *Hscen2*-XPC complex

(Figure 6) [45] because the N-terminal end of MLT is oriented towards the tethered helix of *Crcen*. The electron density map of this crystal structure shows that there are hydrophobic interactions between the N-terminal end of MLT and the tethered helix of *Crcen* [37]. In the amino acids sequence of MLT (discussed above) we can appreciate that the N-terminal end of MLT constitutes primarily hydrophobic residues. Thus, these results confirmed the importance of the hydrophobic interactions between the N-terminal end of MLT and the C-terminal domain of *Crcen*.

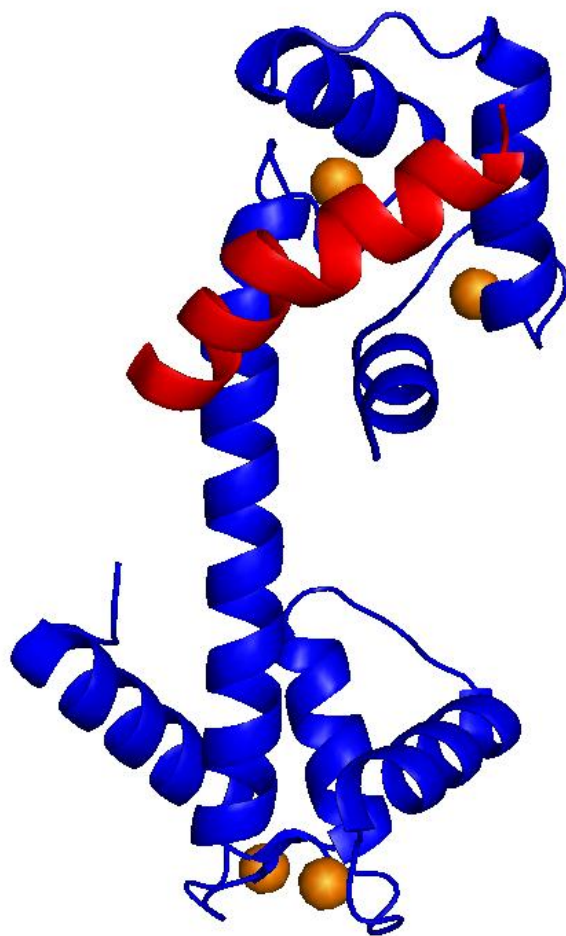


Figure 5. Ribbon structure of *Crcen*-MLT complex (PDB ID 3QRX). In this ribbon representation, *Crcen* is blue, MLT is red and the calcium ions are represented in orange spheres (*Adapted from Sosa et al. 2011 [37]*).

Thermodynamic studies of the *Crcen*-MLT complex were performed at 25°C by Pastrana's group [37] and the results obtained suggested that full-length *Crcen*-MLT complex formation is exothermic (negative enthalpy). By comparing the *Bos taurus* calmodulin-melittin (*BtCaM*-MLT) complex [39] with the *Crcen*-MLT complex, we can see that *Crcen*-MLT complex is more stable and has the highest affinity. However, the enthalpy change result of the *Hscen2*-MLT complex [8] has a more favorable binding than the other complexes mentioned. Finally, complex formation is driven by entropy for the *Crcen*-MLT complex (Figure 6).

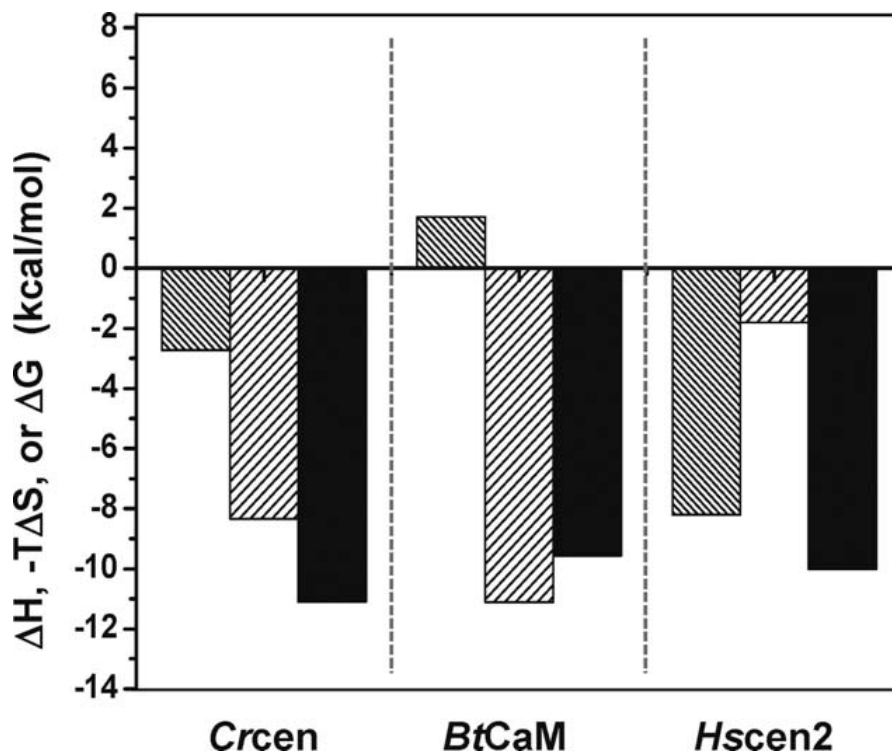


Figure 6. A comparative thermodynamic analysis of CaBP-MLT complexes. Comparison of the change in enthalpy of binding (ΔH_B , narrow striped bars), the change in entropy of binding ($-T\Delta S_B$, wide striped bars), and the Gibbs free energy of binding (ΔG_B , solid bars) for *Crcen*-MLT complex, *BtCaM*-MLT complex, and *Hscen2*-MLT complex at 25, 25, and 30°C and pH 7.4, 7.0, and 6.5, respectively (Adapted from Sosa et al. 2011 [37]).

Centrin-XPC complex

Nucleotide excision repair (NER) is a deoxyribonucleic acid (DNA) repair pathway for damage caused by UV radiation, carcinogens and chemotherapeutic agents. This DNA repair pathway consists of four steps: (1) damage recognition, (2) excision of the damaged DNA, (3) gap-filling by DNA polymerase activity, and (4) ligation [28]. Nishi et al. in 2005 [27] found that in order to stimulate NER, *Hscen2* must interact with XPC in the nucleus. Further studies showed that SUMO 2/3 also interacts with *Hscen2* and influences *Hscen2* localization to the nucleus. Moreover, the interaction between *Hscen2* and XPC is regulated by SUMO 2/3 [29]. Thompson and his co-workers in 2006 [45] characterized the crystal structure of full-length *Hscen2*-XPC complex (Figure 7, PDB ID 2GGM). The *HsXPC* peptide segment used in that experiment was ${}_{847}\text{NWKLLAKGLLIRERLKR}_{863}$. Only residues of the C-terminal domain of *Hscen2* interact with XPC. In Figure 7, *Hscen2* is similar to *Crcen* in that the protein adopts a dumbbell-like shape in which the N-terminal domain does not interact with the C-terminal domain [45]. The interface between *Hscen2* and XPC are extensively hydrophobic. In the sequence alignment shown in Figure 8, the centrin binding sites within XPC for *Homo sapiens*, *Mus musculus*, *Drosophila melanogaster*, *Arabidopsis thaliana*, and *Saccharomyces cerevisiae*, a well conserved tryptophan (W_{848}) is observed at position 848 within the sequence. Taking the tryptophan as the first position; there are also highly conserved leucines (L_{851} and L_{855}) at the fourth and eighth positions, respectively. This is

called the hydrophobic triad with the centrin binding motifs 1-4-8. This hydrophobic triad (W₁L₄L₈) in the centrin binding site of XPC fits in the hydrophobic pocket located in the C-terminal domain of *Hscen2* [9, 45]. In the complex, the *HsXPC* peptide forms the α -helical coiled-coil conformation. The highly conserved W₁L₄L₈ residues are situated on the same side of the α -helix (Figure 9).

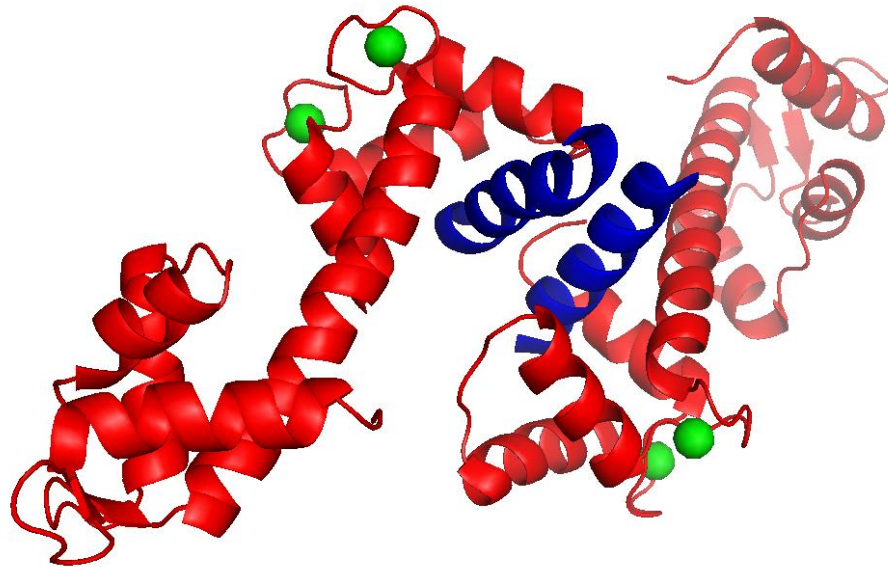


Figure 7. Ribbon structure of *Hscen2*-XPC complex (PDB ID 2GGM). *Hscen2* is red and XPC is blue. The C-terminal domain of *Hscen2* interacts with the XPC peptide (Adapted from Thompson et al. 2006 [45]).

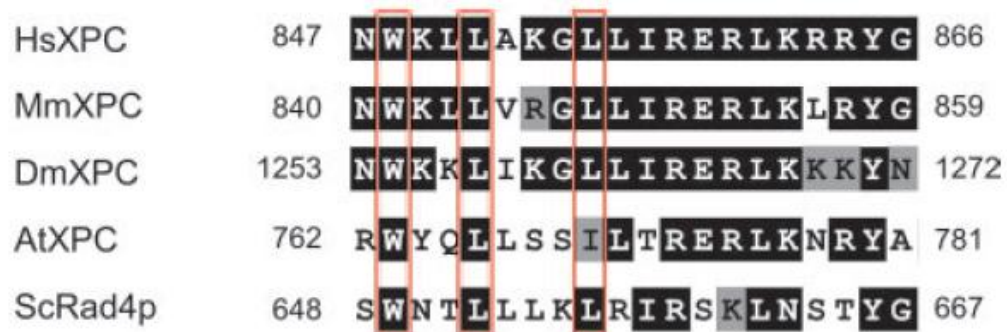


Figure 8. Sequence alignment of the centrin binding sites within XPC in five organisms. Evolutionary conservation of amino acid sequence of the putative centrin 2-binding domain among XPC homologs of *Homo sapiens* (Hs), *Mus musculus* (Mm), *Drosophila melanogaster* (Dm), *Arabidopsis thaliana* (At), and *Saccharomyces cerevisiae* (Sc). The black shade presents identical amino acids in each organism, gray shaded represents conserved mutations and the red boxes identify the hydrophobic triad with the positions 1, 4, and 8 (Adapted from Nishi et al. 2005 [27]).

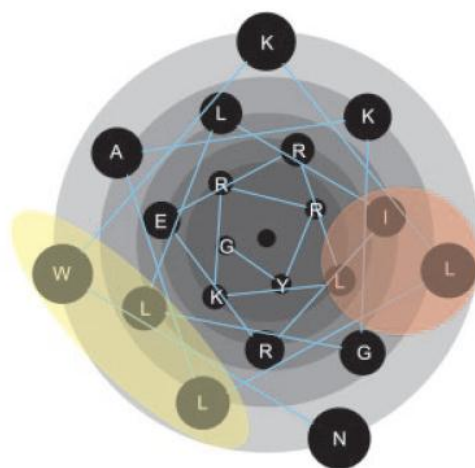


Figure 9. Helical wheel plot of the centrin binding site of XPC. The hydrophobic triad W₁L₄L₈ is located in the same side of the α -helix (*Adapted from Nishi et al. 2005 [27]*).

Centrin-Kar1 complex

Kar1 is another known biological target for centrin [46]. Like yeast centrin, Kar1 is an essential component of the SPB. Biggins et al. in 1994 [46] showed that one of the functions of Kar1 is to localize Cdc31 to the SPB. Schiebel and colleagues in 1995 [47] identified Kar1_{p239-257} as the centrin binding site in Kar1. This peptide binds with high affinity only to the C-terminal domain of *Crcen* (C-*Crcen*) [48]. Figure 10 presents the structure of the C-*Crcen* - Kar1p complex. In the absence of C-*Crcen*, the Kar1p is a random coil; but during the interaction with centrin this peptide undergoes a conformational change to a helical secondary structure [9, 49]. These results are consistent with the ITC experiments carried out by Craescu's group [44, 50] where a negative entropy change (unfavorable entropic contribution) was found between the interaction of centrin and Kar1p. Figure 11A show that the hydrophobic residues Trp10, Leu13, and Leu14 of Kar1 are the key anchors which interact with the hydrophobic cavity located in C-*Crcen*. Trp10 is buried completely in the hydrophobic cavity of C-*Crcen* [7]. By fluorescence experiments, Chazin's group shows that Ca⁺² induced exposure of hydrophobic cavity of C-*Crcen* for the binding of Kar1p [49].

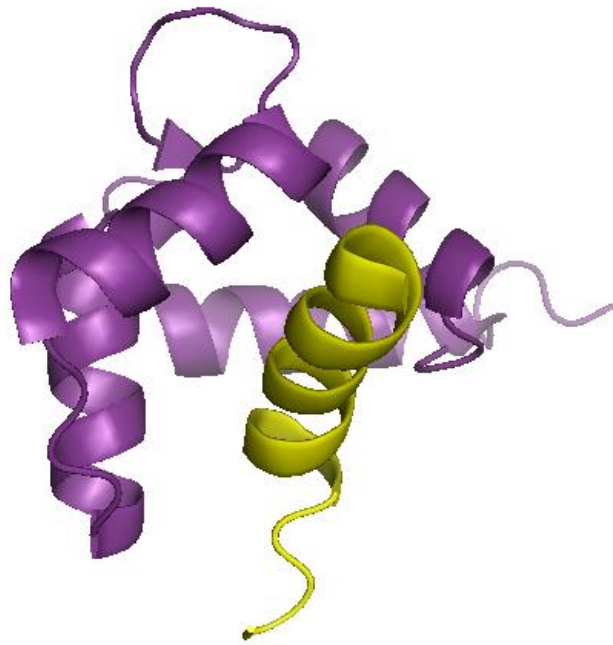


Figure 10. Ribbon structure of C-Crcen-Kar1p complex (PDB ID 1OQP). Kar1p (yellow) interact with the C-terminal domain of Crcen (purple). During the interaction, Kar1p adopts an α -helix secondary structure (*Adapted from Hu and Chazin 2003 [7]*).

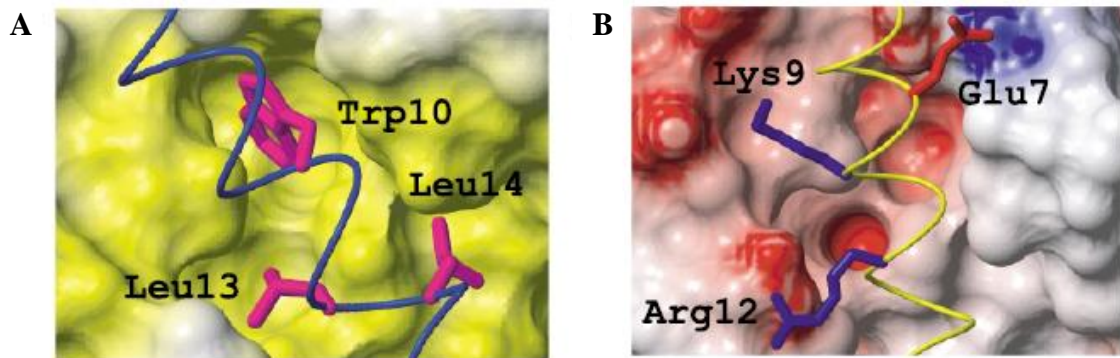


Figure 11. Key interactions stabilizing the complex of C-Crcen with Kar1p. **(A)** Representation of the interaction Trp10, Leu13, and Leu14 hydrophobic residues of Kar1p with the hydrophobic cavity of C-terminal domain of Crcen. **(B)** Electrostatic interaction in the binding interface between Crcen and Kar1p (*Adapted from Hu and Chazin 2003 [7]*).

Sac3-Cdc31-Sus1 ternary complex

TREX-2 is a mRNA export complex consisting of Sac3, Thp1, Sus1, and the centrin homolog (Cdc31) in yeast. Thus, Cdc31 has a role in yeast mRNA export by interacting with the Sac3-Thp1-Sus1 complex. Previous studies show that the interaction between Sac3, Cdc31, and Sus1 is important in order to promote nuclear pore complex (NPC) association of TREX-2 and an efficient mRNA exporter. The structure of the ternary complex Cdc31-Sac3-Sus1 has recently been determined by Jani et al. in 2009 [52]. Cdc31 interacts specifically with Sac3 (Figure 12) [28, 51, 52]. In Figure 13A we can see that the centrin binding site of Sac3 also contains hydrophobic residues in position 1 and 4. Position 1 is occupied by a well conserved tryptophan residue consistent with other centrin binding sites (CBS) i.e., MLT, XPC, and Kar1 discussed above.

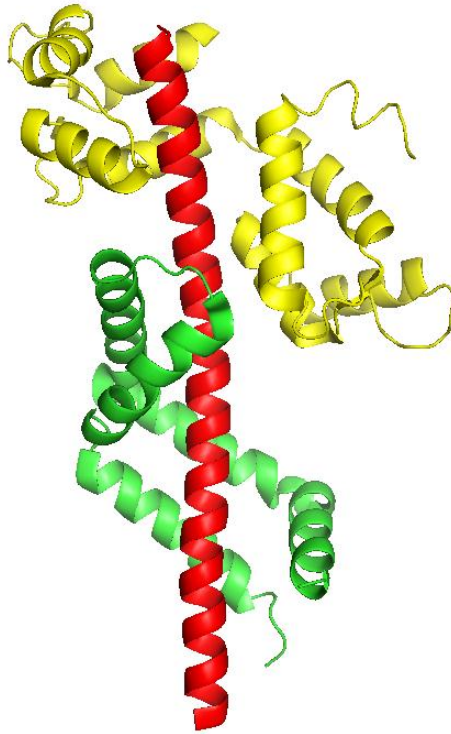


Figure 12. Ribbon structure of Sac3-Cdc31-Sus1 ternary complex (PDB ID 3FWB). Cdc31 is yellow, Sac3 is red and Sus1 is green. In this ternary complex, Cdc31 interact specifically with Sac3 (*Adapted from* Jani et al. 2009 [52]).

In 2011, Miron and his co-workers [50] carried out thermodynamics studies of the Cdc31-ScSac3 complex by isothermal titration calorimetry. Figure 13B shows the thermogram of the interaction between Cdc31 and the ScSac3p (Sac3 peptide $_{797}$ KFFEKWQASYSQAKNRI $_{814}$) at 30°C. This thermogram exhibit a single site interaction which is exothermic ($\Delta H = -25.4$ kcal/mol). The interaction between Cdc31 and Sac3p shows that each single Sac3 centrin binding site can bind one molecule of centrin with a high affinity constant ($K_a = 2.2 \times 10^7$ M $^{-1}$) [48]. Also, fluorescence experiments carried out by this group [48] show that the tryptophan located in position 802 of Sac3p is embedded in an apolar environment from Cdc31. Together, these results show that hydrophobic residues found in the N-terminal end of this peptide of ScSac3 are critical in the interaction between Cdc31 and ScSac3.

A

	1	4	8	17
R18-ScSfi1-20 (680-699) (inverted)	R	F	KK	LVMKELQYNRKSIAQI
R19-ScSfi1-20 (710-729) (inverted)	K	W	IY	FTKVLVFEERVEDALE
R17-hSfi1-20 (641-660) (inverted)	T	V	W	AQLARHLVSHQHHL DAR
R17-hSfi1-12 (649-660) (inverted)	T	V	W	AQLARHLVS
P19-ScKAR1 (237-255)				KKRELIESKWHRLLFHDKK
P18-ScSac3 (797-814) (inverted)	I	R	N	KKAKSYSAGWKEFFK

B

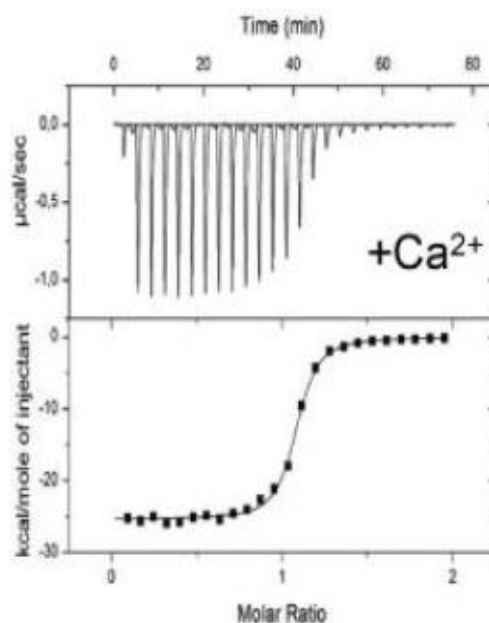


Figure 13. Analysis of the interaction between Cdc31 with Sac3p. **(A)** Amino acid sequence of the centrin binding sites of many biological targets, including Sac3p. **(B)** ITC thermograms and isotherms (at 30°C) of binding of Sac3p with Cdc31 (*Adapted from Miron et al. 2011 [50]*).

Sfi1, a centrin binding protein first identified in yeast

Sfi1 is a protein that was discovered by Ma et al. in 1999 in *Saccharomyces cerevisiae* (Sc) [53]. Sfi1 is an essential protein for the G₂/M transition within the cell cycle [1, 53]. In yeast Sfi1, like Cdc31 (centrin homolog), is localized to the half bridge within the spindle pole body (SPB). Early studies show that there is a lack of homology in the N-terminal and C-terminal domains of Sfi1 in different species [2]. By pull down experiments, Kilmartin in 2003 [1] published his *in vivo* and *in vitro* results confirming that Sfi1 interacts with centrin. In *Homo sapiens* Sfi1 (HsSfi1) and *Saccharomyces cerevisiae* Sfi1 (ScSfi1), there are 23 and 17 tandem centrin binding sites, respectively. These centrin binding sites have the consensus sequence AX₇LLX₃F/LX₂WK/R where the X represents any residue (Figure 14). The gap distance between the centrin binding sites in ScSfi1 is between 23 and 35 residues [1-2]. In the case of HsSfi1, the gap distance between the centrin-binding sites is about 10 amino acids [4]. This short distance gap between centrin binding sites allows centrins to interact with one another [2, 54]. Craescu and his co-workers carried out studies of the interaction between centrin fragments and Sfi1p by ITC and showed that the binding affinity between centrin and Sfi1p is moderately dependent of calcium concentrations [4-5]. In 2006, Li et al. [54] published the structure of Cdc31-ScSfi1 complex (Figure 15). The fragment of ScSfi1 presented in Figure 15 consists of the 2nd, 3rd, and 4th centrin binding sites (N₂₁₈ through H₃₀₆). Each centrin binding site interacts with one centrin. This figure

also shows that the N-terminal domain of Cdc31 interacts with the N-terminal half of ScSfi1, whereas the C-terminal domain of Cdc31 interacts with the C-terminal half of ScSfi1. In the Sfi1p centrin binding site (comprised of only 23 residues), one of the most conserved residues is a tryptophan situated within the C-terminal end of each centrin binding site (Figure 16). Fluorescence and NMR studies made by Craescu's group [4] show that the tryptophan residue located in the C-terminal end of the Sfi1 centrin binding site interacts with the hydrophobic surface situated in the C-terminal domain of centrin 2 including residues 94-172. The centrin binding site seen for XPC [45] with the 1-4-8 type is also present in Sfi1p₁₇ [4]. But, contrary to XPC, the centrin binding sites of Sfi1 flipped orientation for comparison purposes from C-terminal to the N-terminal end (positions 8, 4, and 1) [1, 4-5]. In the centrin binding sites, the first and fourth are always occupied with hydrophobic residues but the eighth position is less conserved because it can be hydrophobic, but also have charged or polar residues (Figure 13A).

The interaction between centrin and Sfi1 has an essential role in SPB duplication. The N-terminal of Sfi1 is associated with the mother SPB. Kilmartin's group proposed in 2006 [54] that during the SPB duplication, the half bridge elongates through tail-to-tail binding and assembly of the centrin-Sfi1 fibers. This binding is mediated by the Sfi1 C-terminal of the older and newer centrin-Sfi1 fibers. Thus, the half bridge provides an anchor site at the N-terminal of the new

centrin-Sfi1 fiber where a satellite structure forms which initiates the assembly of a new daughter SPB. Thus, this 'bridge' allows the connection of between the two SPBs. (Figure 14) [3, 54].

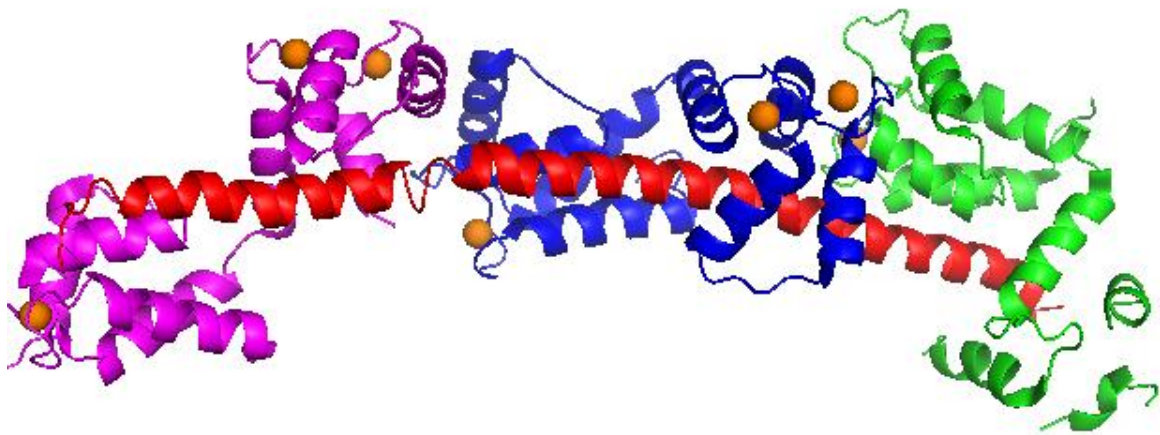


Figure 15. Ribbon structure of Cdc31-ScSfi1 complex (PDB ID 2DOQ). In this complex, we can see three centrin binding sites in Sfi1 (N₂₁₈ through H₃₀₆) that interact with three centrins (purple, blue, and green) with Ca⁺² bound (orange spheres) (*Adapted from Li et al. 2006 [55]*).

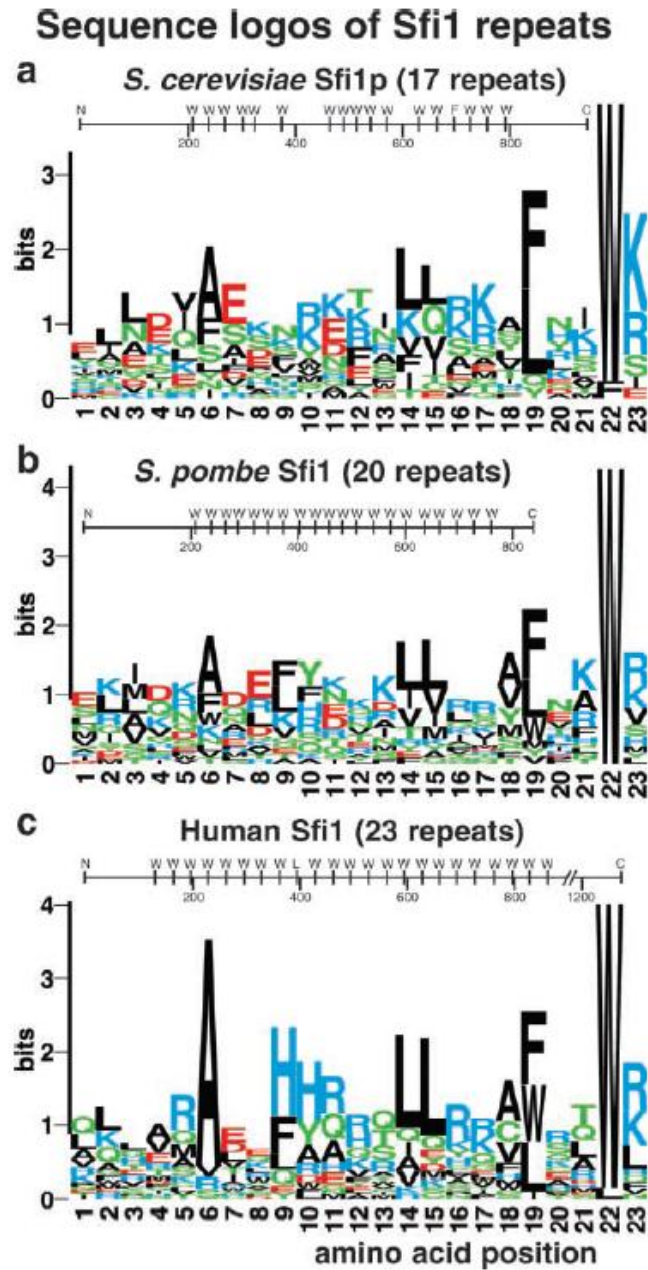


Figure 16. Sequence logos of Sfi1 repeats in *S. cerevisiae* and potential homologues in *S. pombe* (*SpSfi1*), *H. sapiens* (*HsSfi1*) (Adapted from Kilmartin 2003 [1]).

Isothermal Titration Calorimetry

ITC is a powerful tool to carry out thermodynamic studies of protein-protein interactions. The reaction cell in the ITC contains one of the reactants; the titrant is added by injection in small volumes, and stirred. The reference cell contains the buffer or water without the macromolecule. The amount of power needed to maintain a constant temperature difference between a reaction cell and the reference cell during the titration is measured by the calorimeter (Figure 17). These two cells are surrounded by an adiabatic jacket. Heaters located on the reference cell, reaction cell and the jacket are activated when necessary to maintain identical temperature between all components [55]. Thus, the heat absorbed (endothermic) or released (exothermic) by the chemical reaction is obtained from the integral of the power curve over the appropriate time (Figure 18) [56]. For an exothermic reaction, the temperature in the reaction cell will increase, and the feedback power will be deactivated to preserve equal temperatures between the reaction cell and the reference cell. For an endothermic reaction, the reverse will occur. In Figure 18A, each peak corresponds to one injection and Figure 18B represents the integral heat effect due to the binding as a function of the molar ratio. In this figure we can see an exothermic reaction where the peaks are progressively smaller with each injection. This is because there is less free protein available for binding. When the protein is saturated, the peak height represents the background level. It is

important to note that the heat absorbed or released during an ITC experiment is proportional to the fraction of the bound ligand. For this reason, it is very important to determine the initial concentrations of the protein and the ligand with a high degree of precision.

ITC is a technique that allows simultaneous determination of all binding parameters: the affinity constant (K_a), change in Gibbs free energy (ΔG_B), the change in enthalpy (ΔH_B), the change in entropy (ΔS_B), and the stoichiometry (n) [57]. At a constant temperature (T), the change in Gibbs free energy is given by:

$$\Delta G_B^\circ = -RT \ln K_a = \Delta H_B^\circ - T\Delta S_B^\circ \quad (1)$$

where R is the gas constant. The ITC is the only technique where these parameters can be directly and accurately determined from a single experiment [6]. ΔH_B represents the experimentally measured quantity in calorimetry. The binding enthalpy provides us information about the competition between protein-ligand interactions (e.g. hydrogen bonds, salt bridges, hydrophobic interactions). A favorable enthalpy indicate that the protein established good interactions such as hydrogen bonds, salt bridges, and hydrophobic interactions with its biological target and the interactions are strong enough to compensate the unfavorable enthalpy associated with the loose of the interaction with the surrounding water molecules. A large unfavorable enthalpy means that the polar groups of the

protein lose the interaction with the solvent without being able to form interactions with its biological target [58]. The binding entropy reflects changes in solvation entropy and changes in the conformation of the proteins within the complex entropies. The changes in solvation entropy are favorable when the binding of the biological target occurs with the protein. Thus, favorable solvation entropy is associated with the binding energy of hydrophobic groups. The conformational entropy change is unfavorable when the binding process involves the loss of conformational degrees of freedom of both the protein and its biological target [58]. K_a is a measure of the affinity of the interaction. ΔG_B can give us information about the stability of the complex [59]. Figure 19 illustrate the components of the binding energy involved in the interaction between a small molecule and its target. The stoichiometry is determined from the titration equivalence point (Figure 18B). In addition, by repeating the titration at different temperatures, we can determine the change in binding heat capacity (ΔC_p) during the reaction:

$$\Delta C_p = \frac{\partial \Delta H}{\partial T} \quad (2)$$

ΔC_p has been used to estimate the amount of polar and nonpolar surface buried on formation of the complex [56]. The increase in ΔC_p is caused by the hydration change of proteins. The change in hydration is closely related to change in polar and nonpolar solvent accessible area [60].

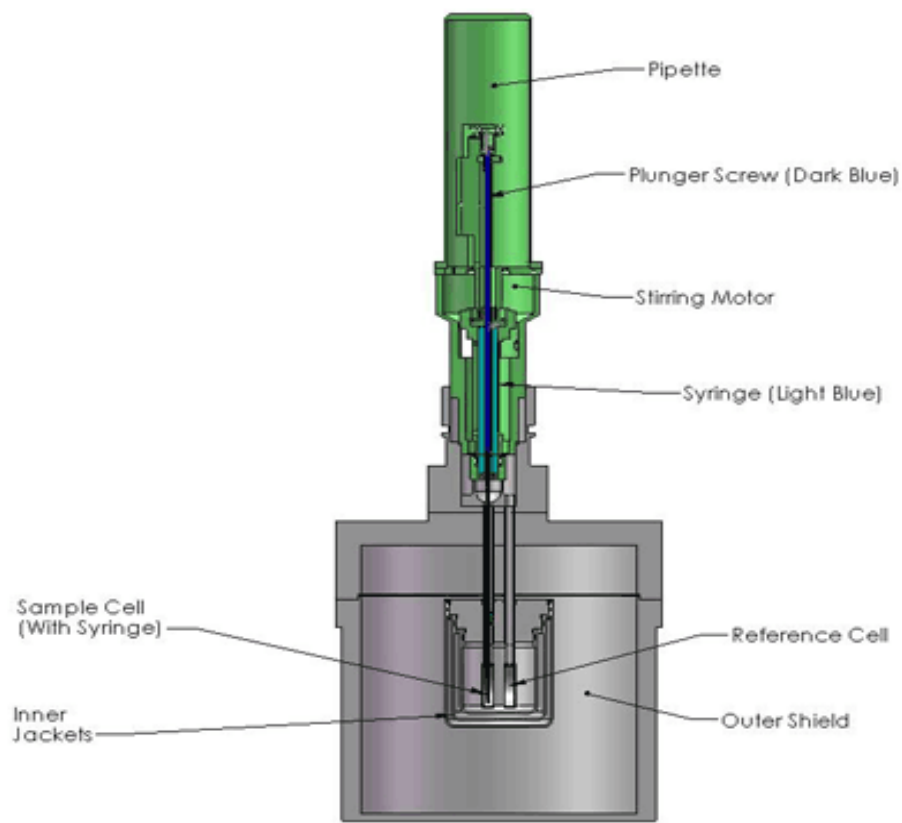


Figure 17. Diagram of ITC cells and syringe. The sample cell and the reference cell are contained within the adiabatic jacket. The ITC measures the heat as a function of time that must be added to the sample cell in order to maintain a temperature difference equal to zero between the two cells at the designated temperature for an experiment (<http://www.microcal.com/technology/itc.asp>).

Isothermal Titration Calorimetry (ITC)

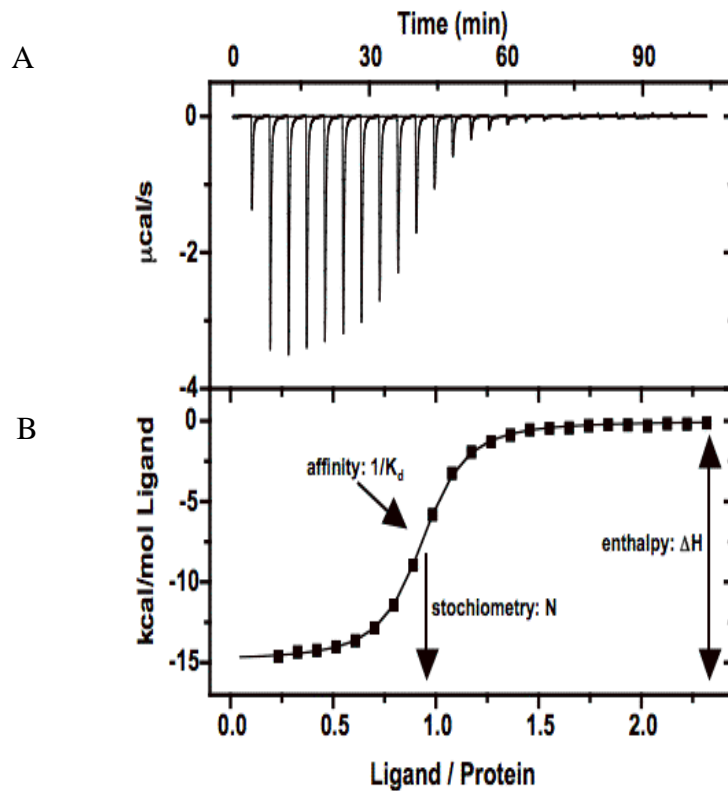


Figure 18. Representation of ITC data. **(A)** The upper panel is the power data and **(B)** the lower panel is the integrated enthalpy. (<http://www.endocytosis.org/techniqs/ITC.html>)

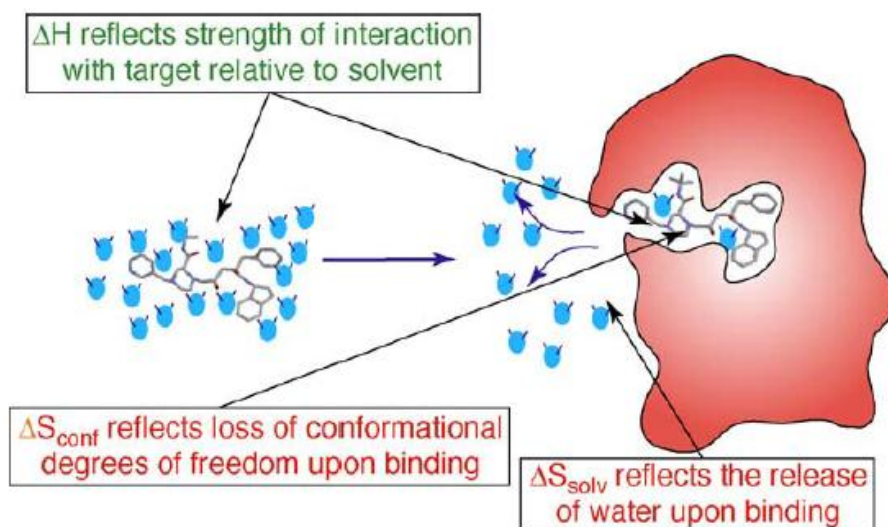


Figure 19. Illustration of the binding energy involved in an interaction between a small molecule (red) and its target. The change in enthalpy (ΔH) reflects strength of interaction with target relative to solvent, i.e. water (cyan). The change in entropy reflects changes in solvation entropy (ΔS_{solv}) and changes in conformation of the molecule (ΔS_{conf}) (Adapted from Freire 2004 [58]).

CHAPTER III

MATERIALS AND METHODS

Protein and Peptide Preparation

Wild type of centrins were expressed, isolated, and purified following a protocol established in our laboratory as previously described [61]. The peptide (*HsSfi1p₂₁*: AQQLQLERAVQHHRQLLLEGLARWKTHLLQ) was purchased from Abgent (San Diego, CA). The Mass Spectrometry (MS) and the High Performance Liquid Chromatography (HPLC) results carried out by Abgent were included in this thesis to presents the molecular mass and the purity of *HsSfi1p₂₁*. In order to remove the trifluoroacetic acid (TFA) from the peptide, 100 μ L of HCl 0.1 M was added to the peptide and then lyophilized. Then, in order to remove the HCl from the peptide, 100 μ L of deionized water was added to the peptide and then lyophilized (this procedure was repeated four consecutive times). Protein and peptide concentrations were determined using a JASCO model V-560 UV/Vis Spectrophotometer. The extinction coefficient (ϵ) of *Hscen1* and *Hscen2* is 1,490 $M^{-1}cm^{-1}$ at 280 nm; the ϵ of *Hscen3* and *HsSfi1p₂₁* are 8,480 $M^{-1}cm^{-1}$ and 5,500 $M^{-1}cm^{-1}$ at 280 nm, respectively.

Isothermal Titration Calorimetry:

Titration experiments were carried out using a VP-ITC microcalorimeter (MicroCal LLC, Northampton, MA). The buffer for all experiments was 50 mM HEPES, 150 mM NaCl, 4 mM CaCl₂, and 4 mM MgCl₂ at pH 7.4. The experimental temperatures were 25 °C, 30 °C, 35 °C, and 40 °C. The protein and peptides of interest were exhaustively dialyzed against the buffer of choice prior to the isothermal titration experiments using a dialysis membrane (Spectrum Laboratories, Inc.) with a cutoff of 500 Da. Typical concentrations of *Hscen1* and *Hscen3* ranged between 100-224 μM and 48-64 μM, respectively. The concentration of *Hscen2* used in this experiment was 112 μM. The peptide concentration ranged between 8-10 μM. All the solutions were degassed for at least 10 min prior to use.

Analysis of ITC Data

The ITC power data was integrated and analyzed using MicroCal Origin software, and values for the change in enthalpy of binding (ΔH_B), the change in entropy (ΔS_B), the association constant (K_a) and the stoichiometry of the binding (n) were determined. The change of in Gibbs free energy (ΔG_B) was calculated using equation (1). ΔC_p was obtained by the linear best fit of the ΔH versus temperature data.

Crystallization Assay

Crystals were grown using the hanging drop vapor diffusion method at room temperature. The crystals presented in Figure 28 were obtained by mixing 2 μL of *Hscen1-HsSfi1p₂₁* (0.150 mg/mL, 1:1.5 mole ratio) solution with 2 μL of a precipitant solution containing 50% (v/v) 2-methyl-2,4-pentanediol (MPD) in 0.1 M Tris pH 8.5. These crystals appeared after seven weeks. In this pre-screening assay, QIAGEN[®] EasyXtal Pre-screen Assay (QIAGEN Inc., Valencia, CA) was used. This pre-screen assay contained 24 different precipitants in solution (Table 1)

Table 1. QIAGEN® EasyXtal pre-screen suite composition table.

Well	Chemical 1	Chemical 2	Buffer
A1	4.3 M Sodium chloride		
A2	1.5 M Sodium chloride		
A3	30% (v/v) Glycerol	2 M Ammonium sulfate	
A4	15% (v/v) Glycerol	2 M Ammonium sulfate	
A5	30% (v/v) PEG 400		
A6	15% (v/v) PEG 400		
B1	3.2 M Ammonium sulfate		
B2	1.1 M Ammonium sulfate		
B3	40% (v/v) 2-propanol		
B4	15% (v/v) 2-propanol		
B5	30% (w/v) PEG 4000		
B6	12% (w/v) PEG 4000		
C1	3 M Na/K phosphate pH 7.0		
C2	1 M Na/K phosphate pH 7.0		
C3	65% (v/v) MPD		
C4	23% (v/v) MPD		
C5	30% (w/v) PEG 8000		
C6	12% (w/v) PEG 8000		
D1	2 M Ammonium sulfate		0.1 M Sodium acetate pH 4.6
D2	2 M Ammonium sulfate		0.1 M Tris pH 8.5
D3	50% (v/v) MPD		0.1 M Sodium acetate pH 4.6
D4	50% (v/v) MPD		0.1 M Tris pH 8.5
D5	20% (w/v) PEG 4000		0.1 M Sodium acetate pH 4.6
D6	20% (w/v) PEG 4000		0.1 M Tris pH 8.5

Abbreviations:

PEG = Polyethylene glycol

MPD = 2-methyl-2,4-pentanediol

The crystals presented in Figure 29 were obtained by mixing 2 μL of *Hscen1-HsSfi1p₂₁* (15.9 mg/mL total protein, 1:1.5 mole ratio) solution with 2 μL 50% (v/v) MPD in 0.1 M sodium acetate. The crystal shown in Figure 30 was obtained by mixing 1 μL of *Hscen1-HsSfi1p₂₁* (15.9 mg/mL total protein, 1:1.5 mole ratio) solution with 1 μL 40% (v/v) 2-propanol. These crystals presented in Figures 29 and 30 appeared after 2-5 days. These precipitant solutions were prepared using the highest purity reagents commercially available in the Pastrana laboratory. The precipitating agents were all purchased from Hampton Research (Aliso Viejo, CA). The precipitant solutions used in this assay are presented in Table 2 (A and B).

Table 2. Pre-screen assay suite composition tables (A and B). These precipitant solutions were prepared in Dr. Pastrana's Laboratory.

A

Well	Chemical	Buffer
A1	10% PEG 4000	0.1 M Sodium acetate pH 4.6
A2	15% PEG 4000	0.1 M Sodium acetate pH 4.6
A3	20% PEG 4000	0.1 M Sodium acetate pH 4.6
A4	25% PEG 4000	0.1 M Sodium acetate pH 4.6
A5	20% 2-propanol	0.1 M Sodium acetate pH 4.6
A6	35% 2-propanol	0.1 M Sodium acetate pH 4.6
B1	40% 2-propanol	0.1 M Sodium acetate pH 4.6
B2	40% MPD	0.1 M Sodium acetate pH 4.6
B3	45% MPD	0.1 M Sodium acetate pH 4.6
B4	50% MPD	0.1 M Sodium acetate pH 4.6
B5	10% PEG 4000	0.1 M HEPES pH 7.4
B6	15% PEG 4000	0.1 M HEPES pH 7.4
C1	20% PEG 4000	0.1 M HEPES pH 7.4
C2	25% PEG 4000	0.1 M HEPES pH 7.4
C3	20% 2-propanol	0.1 M HEPES pH 7.4
C4	35% 2-propanol	0.1 M HEPES pH 7.4
C5	40% 2-propanol	0.1 M HEPES pH 7.4
C6	40% MPD	0.1 M HEPES pH 7.4
D1	45% MPD	0.1 M HEPES pH 7.4
D2	50% MPD	0.1 M HEPES pH 7.4
D3	20% 2-propanol	
D4	35% 2-propanol	
D5	40% 2-propanol	

B

Well	Chemical	Buffer
A1	10% PEG 4000	0.1 M Tris pH 8.5
A2	15% PEG 4000	0.1 M Tris pH 8.5
A3	20% PEG 4000	0.1 M Tris pH 8.5
A4	25% PEG 4000	0.1 M Tris pH 8.5
A5	20% 2-propanol	0.1 M Tris pH 8.5
A6	35% 2-propanol	0.1 M Tris pH 8.5
B1	40% 2-propanol	0.1 M Tris pH 8.5
B2	40% MPD	0.1 M Tris pH 8.5
B3	45% MPD	0.1 M Tris pH 8.5
B4	50% MPD	0.1 M Tris pH 8.5

Abbreviations discussed above.

CHAPTER IV

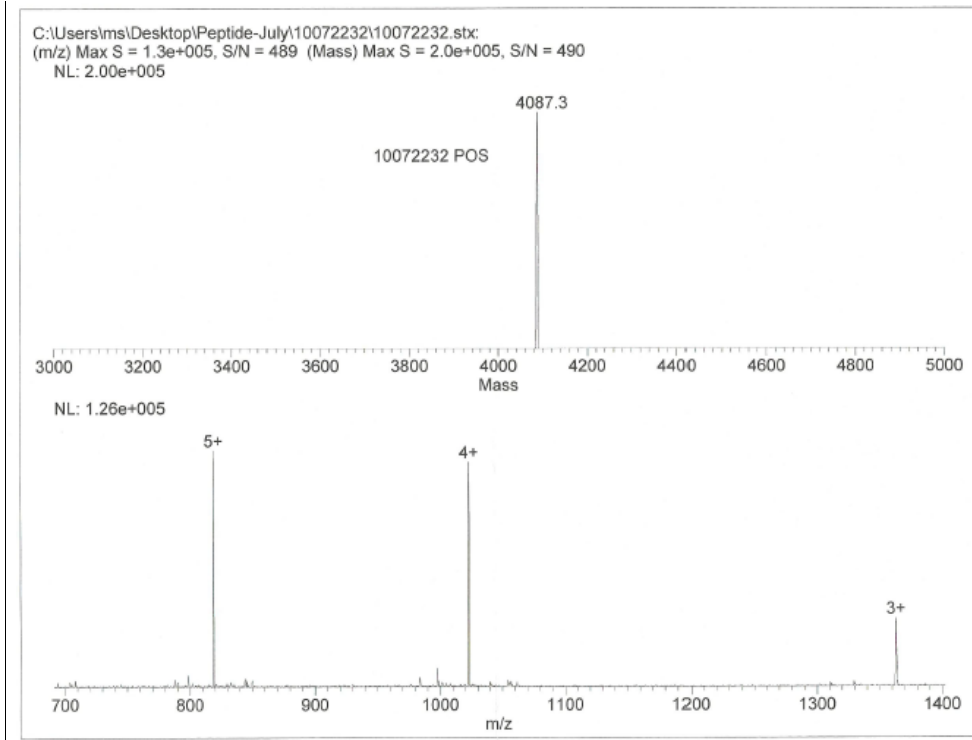
RESULTS AND DISCUSSIONS

Analysis of *HsSfi1p₂₁*

Mass Spectrometry and High Performance Liquid Chromatography

The molecular weight and the purity *HsSfi1p₂₁* (Acetyl-AQRLQLERAVQHHRQLLLEGLARWKTHLLQ-NH₂) were determined by Mass Spectrometry (MS) and High Performance Liquid Chromatography (HPLC) analyses, respectively. These analyses were carried out by Abgent after the synthesis of this peptide. The calculated molecular weight for *HsSfi1p₂₁* is 4086.57 Da while the experimental molecular weight obtained by the MS report was 4087.3 Da (Figure 20A). The purity of *HsSfi1p₂₁* obtained by the HPLC report was >95% (Figure 20B). Thus, these results show that the *HsSfi1p₂₁* purchased has a high purity.

A



B

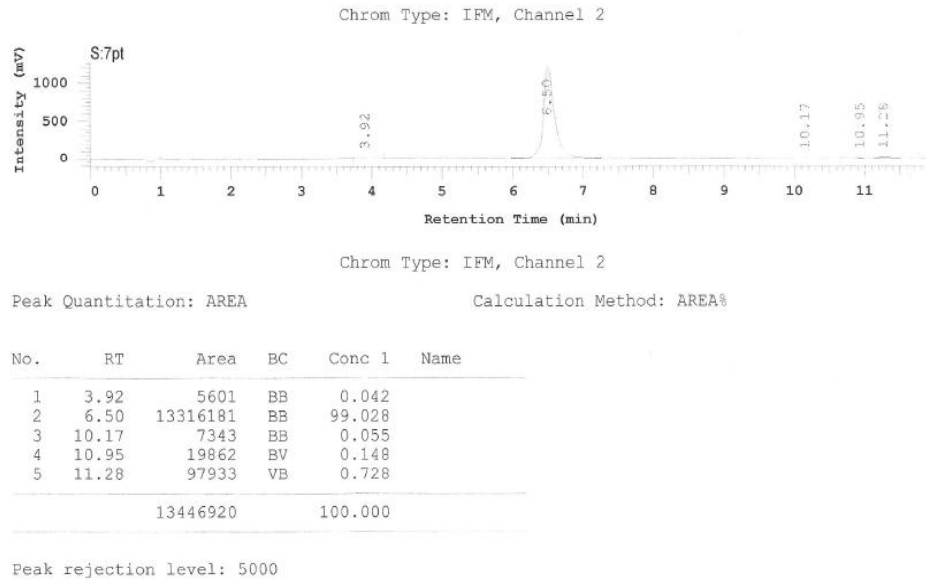


Figure 20 Mass Spectrometry and HPLC results from *HsSfi1p₂₁*. **(A)** Mass Spectrometry report showed that the molecular weight of *HsSfi1p₂₁* was 4087.3 m/z. **(B)** HPLC results confirmed that *HsSfi1p₂₁* was obtained with >95%.

***HsSfi1p₂₁* sequence analysis.**

Homo sapiens Sfi1 full-length protein is comprised of 1242 amino acids and contains twenty three tandem centrin binding sites, as shown in Figure 21A. The 21st centrin binding site of Sfi1 was chosen in order to characterize the thermodynamic features of the interaction between centrin and this peptide. Figure 21B presents a comparison of the sequence of *HsSfi1p₂₁* with Sfi1's centrin binding sites previously studied [4]. In the sequence of *HsSfi1p₂₁* we can note the consensus motifs AX₇LLX₃F/LX₂WK/R presented by Kilmartin [1]. Also, *HsSfi1p₂₁* has various polar and charged residues. As a result, *HsSfi1p₂₁* is a soluble peptide. Figure 21C depicts the sequence alignment of *HsSfi1p₂₁* and known centrin binding peptides. Some peptides are in an inverted representation (C-terminal end to N-terminal end) in order to highlight the conserved hydrophobic residues. These residues located in positions 1, 4, and 8 represent the hydrophobic residues found to be important for the interaction between centrin and Sfi1p. The first position is occupied with the well conserved tryptophan. The first and fourth are always occupied with hydrophobic residues but the eighth position is less conserved because it can be hydrophobic but also charged or polar residues. As discussed in the previous chapter, in the complex between centrin and its biological targets these hydrophobic residues are in the hydrophobic surface exposed by the C-terminal domain of centrin. Some centrin binding peptides, like *HsSfi1p₂₁* and *HsPOC5p₁₋₃*, also have conserved hydrophobic residues in the 17th position. The

secondary structure of centrin's biological target during the complex is α -helix (Figures 4, 6, 9, 11 and 14). In order to study the localization of these conserved hydrophobic residues in the structure of *HsSfi1p₂₁*, the amino acid sequence of this peptide was plotted as a helical wheel (Figure 22) [62]. In the C-terminal end of *HsSfi1p₂₁*, we can see that the hydrophobic surface consists of the hydrophobic triad W₁L₄L₈. These hydrophobic residues are located in the same side of the α -helix. Together, these results show that the hydrophobic triad W₁L₄L₈ located in the C-terminal end of *HsSfi1p₂₁* is critical for the interaction between centrin and this peptide.

A MKNLLTEKCISSHNHFQKVIKQRMEKKVDSRYFKDGAVKKPYSAKTLSNKKSSASFGIRREL PSTSHLVQ
 YRGHTTCTRQGRRLRELRI RCVARKFLYLWIRMTFGRVFP SKARFYEQRLLRKVFE EWKEEWWVFQHEWK
 LCVRADCHYRYLYLNLMFQ TWKTYVRQQQEMRNKYIRA EVDHAKQKMRQAWKSWLIYVVVRRTKLQMQTT
 ALEFRQRIILRVVWSTWRQRLGQVRVSRALHASALKHRALSLQVQAWSQWREQLLYVQKEKQKVVSAVKH
 HQHWQKRRFLKAWLEYLQVRRVKRQQNEMAERFHHVTVLQIYFCDWQQAWERRESLYAHHAQVEKLARKM
 ALRRAFTHWKHYMLLCAEEAAQFEMAEHHRHSQLYFCFRALKDNVTHAHLQQIRRNLAHQHGVTL LHR
 FWNLWRSQIEQKKERELLPLLHAAWDHYRIALLCKCIELWLQYTQKRRYKQLLQARADGHFQQORALPAAF
 HTWNRLWRWRHQENVLSARATRFHRETLEKQVFSLWRQKMFQHRENRLAERMAILHAERQLLYRSWFMWH
 QQAAARHQEQEWQTVACAHHRHGRLKKAFC LWRESAQGLRTER TGRVRAAEFHMAQLLRWAW SQWRECLA
 LRGAERQKLMRADLHHQHSVLHRALQAVV TYQGRVRSILREVAARESQHNRQLLRGALRRWKENTMARVD
 EAKKTFQASTHYRRTICSKVLVQWREAVSVQMYRQ QEDCAIWEAQKVLDRGCLRTWFORWWDCSRRSAQ
 QRLQLERAVQHHRQLLLEGLARWKTHHLQCVRKRL LHRQSTQLLAQRLSRTCFRQWRQQLAARRQEORA
 TVRALWFWAFSLQAKVWATWLAFLVLERRRKARLQWALQAYQ GQLLEGATRLLRF AASMKASRQQLQAO
 QQVQAAHSLHRAVRRCATLWKQKVLGRGGKQPLAAIAPSRKVT FEGPLLNR IAAGAGDGTLET KRPQAS
 RPLGALGR LAEEPHALELNTAHSARKQPRRPHFLLEPAQSQR POKPQEHGLGMAQPAAPSLTRPFLAEA
 PTALVPHSPLPGALSSAPGPKQPPTASTGPELLLLPLSSFMPCGAAAPARVSAQRATPRDKPPVPSSLAS
 VPDPHLLLPGDFSATRAGPGLSTAGSLDLEAELEEIQ QLLHYQTTKQNLWSCR RQASSLRRWLELNREE
 GPGEDQEVEQQVQKELEQVEMQIQLLAEELQAQRQPIGACVARIQALRQALC

B

Centrin binding site sequence	A	X	X	X	X	X	X	X	L	L	X	X	X	F/L	X	X	W	K/R
HsSfi1p ₁ (112-129)	A	R	F	Y	Y	E	Q	R	L	L	R	K	V	F	E	E	W	K
HsSfi1p ₁₂ (477-494)	A	D	G	H	F	Q	Q	R	A	L	P	A	A	F	H	T	W	N
HsSfi1p ₁₇ (642-659)	A	D	L	H	H	Q	H	S	V	L	H	R	A	L	Q	A	W	V
HsSfi1p ₂₁ (778-795)	A	V	Q	H	H	H	R	Q	L	L	L	E	G	L	A	R	W	K

C

						1		4		8					17																			
<i>HsSfi1p₂₁</i> (769-801) inverted		Q	L	L	H	H	T	K	W	R	A	L	G	E	L	L	L	Q	R	H	H	Q	V	A	R	E	L	Q	L	R	Q	Q	A	
<i>HsXPC</i> (847-863)						N	W	K	L	L	A	K	G	L	L	I	R	E	R	L	K	R												
<i>ScKar1</i> (239-257)		K	K	R	E	L	I	E	S	K	W	H	R	L	L	F	H	D	K	K														
<i>HsPOC5p₁</i> (142-173) inverted		N	T	K	L	G	S	S	W	L	D	L	V	N	E	M	K	Q	L	N	E	D	S	V										
<i>HsPOC5p₂</i> (237-262) inverted		A	R	V	H	G	I	R	W	H	F	F	T	R	M	L	E	I	K	E	K	Q	K	G	I	A	H	S	L	S	S	I	V	
<i>HsPOC5p₃</i> (270-295) inverted		Q	K	Q	V	V	S	R	W	V	K	W	V	K	K	L	L	T	R	Q	Y	Y	Q	D	A	L	K	G	E	Y	V	D	Q	R
<i>MLT</i> (43-64) inverted		Q	K	R	K	N	K	I	W	S	I	L	T	P	L	G	T	A	L	V	K	L	I	A	G	I	G							
<i>ScSac3</i> (797-814) inverted	I	R	N	K	K	A	Q	S	Y	S	A	Q	W	K	E	F	F	K																

Figure 21. Sequence analysis of *HsSfi1p₂₁*. (A) FASTA full-length sequence of *HsSfi1*. (B) Sequence alignment of some centrin binding sites of *Sfi1*. (C) Sequence alignment of known centrin binding peptides including *HsSfi1p₂₁*.

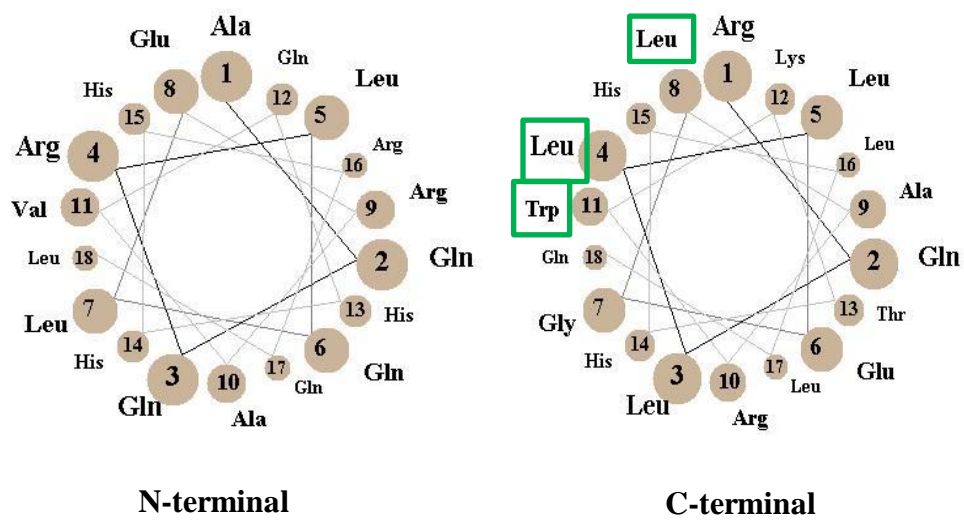


Figure 22. Helical wheel plot of the N-terminal and C-terminal ends of *HsSfi1p*₂₁. The hydrophobic triad W₁L₄L₈ is identified with a box colored in green.

Thermodynamic analyses and crystallization of *Hscen1-HsSfi1p₂₁* complex

The analyses of the interaction between *Hscen1 wild type* (WT) and *HsSfi1p₂₁* were carried out by the ITC. Figures 23-26 present the results of the ITC experiments carried out at 25°C, 30°C, 35°C, and 40°C. At each temperature, the process of the interaction was exothermic (negative enthalpy). Also, in each experiment the stoichiometry of the interaction was always close to 1 which means that only one molecule of centrin binds one molecule of *HsSfi1p₂₁*. The experimental data was best fitted using the single-site binding model. Table 1 summarizes the thermodynamic parameters of the *Hscen1-HsSfi1p₂₁* complex. The interactions that occur in the interface between *Hscen1* and *HsSfi1p₂₁* (such as hydrogen bonding, salt bridges, hydrophobic interactions, etc.) are more favorable ($\Delta H = -29.0$ kcal/mol) at 35°C. The results obtained of $-T\Delta S$ present an unfavorable entropic component ($-T\Delta S = 18.8$ kcal/mol). The main contribution to the negative entropy change is probably because *HsSfi1p₂₁* was undergoing a transition from being a more flexible structure to an ordered, bound structure as a result of the interaction between *Hscen1* and this peptide. The large binding enthalpy and binding entropy compensate the high value of the affinity constant ($K_a = 1.7 \times 10^7$ M⁻¹) and the binding Gibbs free energy ($\Delta G = -10.2$ kcal/mol), thus, indicating highest affinity and stability. Interestingly, this protein-peptide interaction is favorable in a temperature closest to the human body temperature (~37°C). From the analysis of the binding enthalpies as a function of temperature, we can

determine the change in heat capacity (Figure 27). The ΔC_p obtained by the slope was $-0.2524 \text{ kcal/mol } ^\circ\text{C}$. Because there is a relation between change in heat capacity and the burial surface area, these negative ΔC_p may be due to a decrease in exposure of the hydrophobic surface as a result of the interaction between *Hscen1* and *HsSfi1p₂₁*. These results provided the assurance of a stable complex that could be used for the crystallization assays discussed below.

In order to determine and understand the structure of *Hscen1-HsSfi1p₂₁* complex, pre-screen crystallization assays were carried out. Figures 28-30 show the crystal obtained by the hanging drop vapor diffusion method at room temperature. The concentrations of the *Hscen1-HsSfi1p₂₁* complex were 0.150 mg/mL (Figure 28) and 15.9 mg/mL (Figures 29-30) with a 1:1.5 mole ratio. The average size for the micro crystals presented in Figure 28 was $\sim 55 \text{ }\mu\text{m}$, while the size of the crystals presented in Figure 29 and 30 were $158.19 \text{ }\mu\text{m}$ and $201.86 \text{ }\mu\text{m}$, respectively. The crystals shown in Figure 29 are needle shaped.

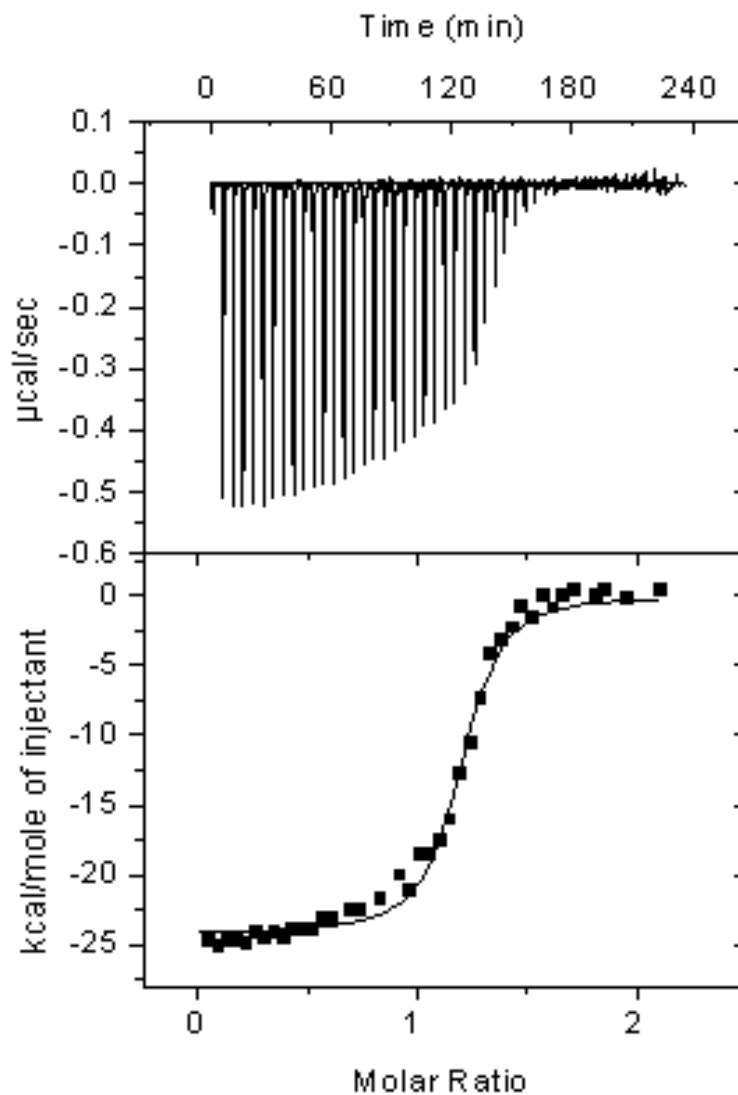


Figure 23. ITC isotherms of the interaction between *Hscen1* (WT) with *HsSfi1p₂₁* at 25°C. The upper panels show the raw data and the lower panels show the integrated enthalpy fitted to a single site-binding model.

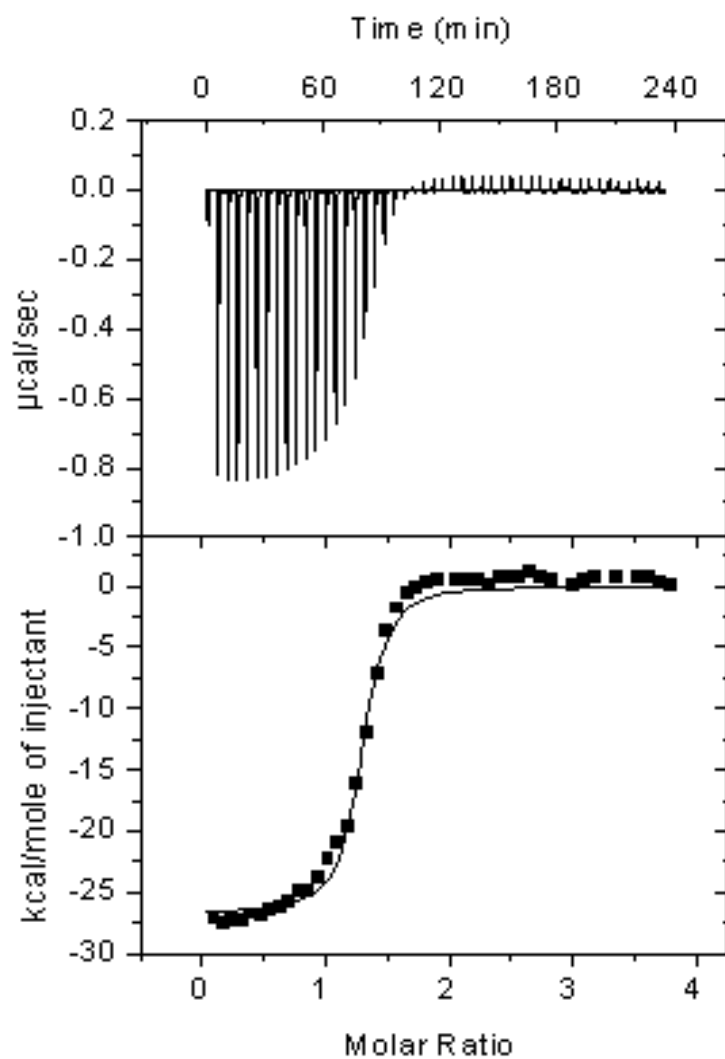


Figure 24. ITC isotherms of the interaction between *Hscen1* (WT) with *HsSfi1p₂₁* at 30°C. The upper panels show the raw data and the lower panels show the integrated enthalpy fitted to a single site-binding model.

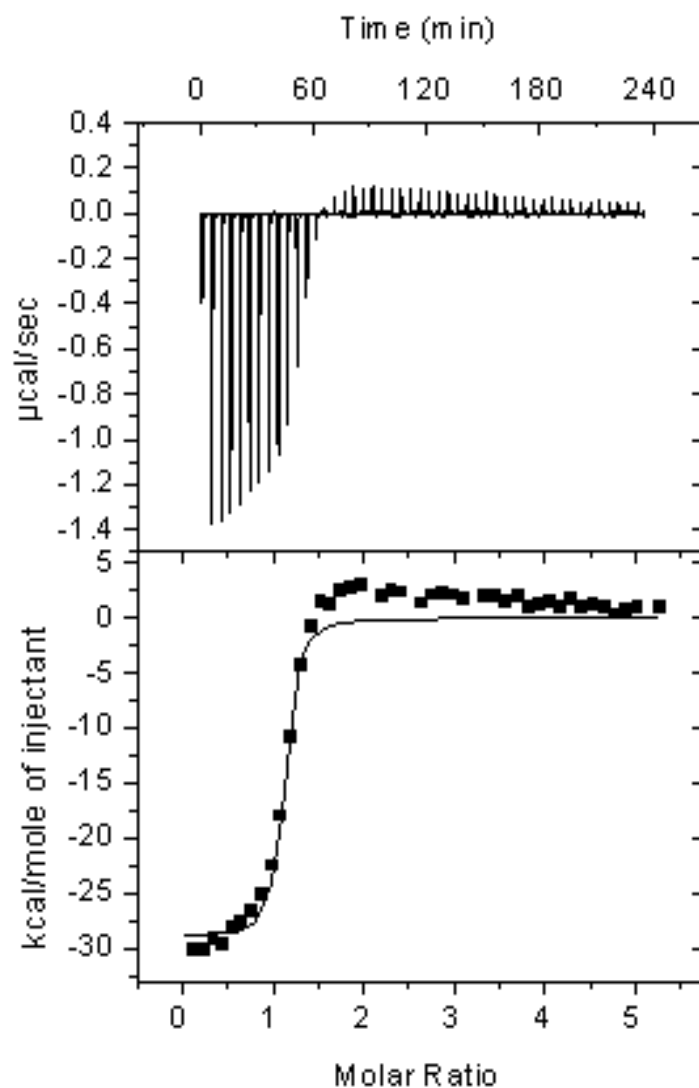


Figure 25. ITC isotherms of the interaction between *Hscn1* (WT) with *HsSfi1p₂₁* at 35°C. The upper panels show the raw data and the lower panels show the integrated enthalpy fitted to a single site-binding model.

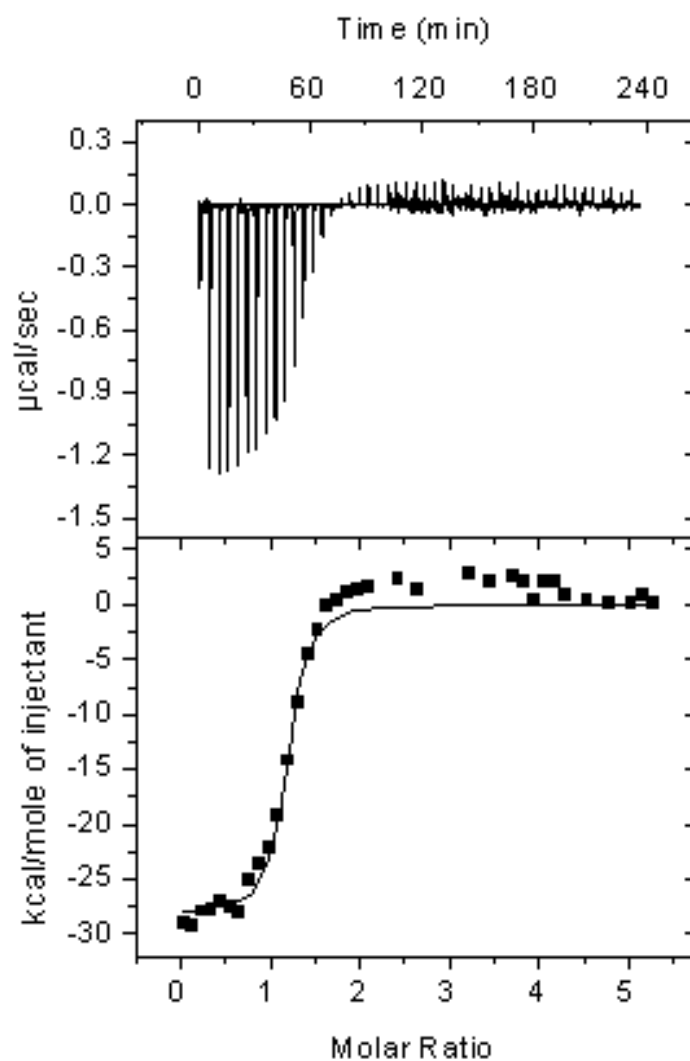


Figure 26. ITC isotherms of the interaction between *Hscen1* (WT) with *HsSfi1p₂₁* at 40°C. The upper panels show the raw data and the lower panels show the integrated enthalpy fitted to a single site-binding model.

Table 3. Summary of the thermodynamic data of the interaction between *Hscen1* (WT) and *HsSfi1p₂₁* at 25 °C, 30 °C, 35 °C, and 40 °C. The stoichiometry of binding is always close to 1.

Temperature (°C)	K _a (error) (10 ⁷ M ⁻¹)	ΔG (kcal/mol)	ΔH (error) (kcal/mol)	-TΔS (kcal/mol)
25	1.5 (0.1)	-9.8	-24.2 (0.1)	14.5
30	1.6 (0.2)	-10.0	-26.7 (0.2)	16.7
35	1.7 (0.6)	-10.2	-29.0 (0.7)	18.8
40	1.0 (0.3)	-10.1	-28.1 (0.6)	18.1

Note: The ITC profile was rendered the best fit when the Chi-squared (Chi²) value obtained range within 10⁵-10⁶.

Binding enthalpies of *Hscen1* (WT) – *HsSfi1p*₂₁ complex as a function of temperature

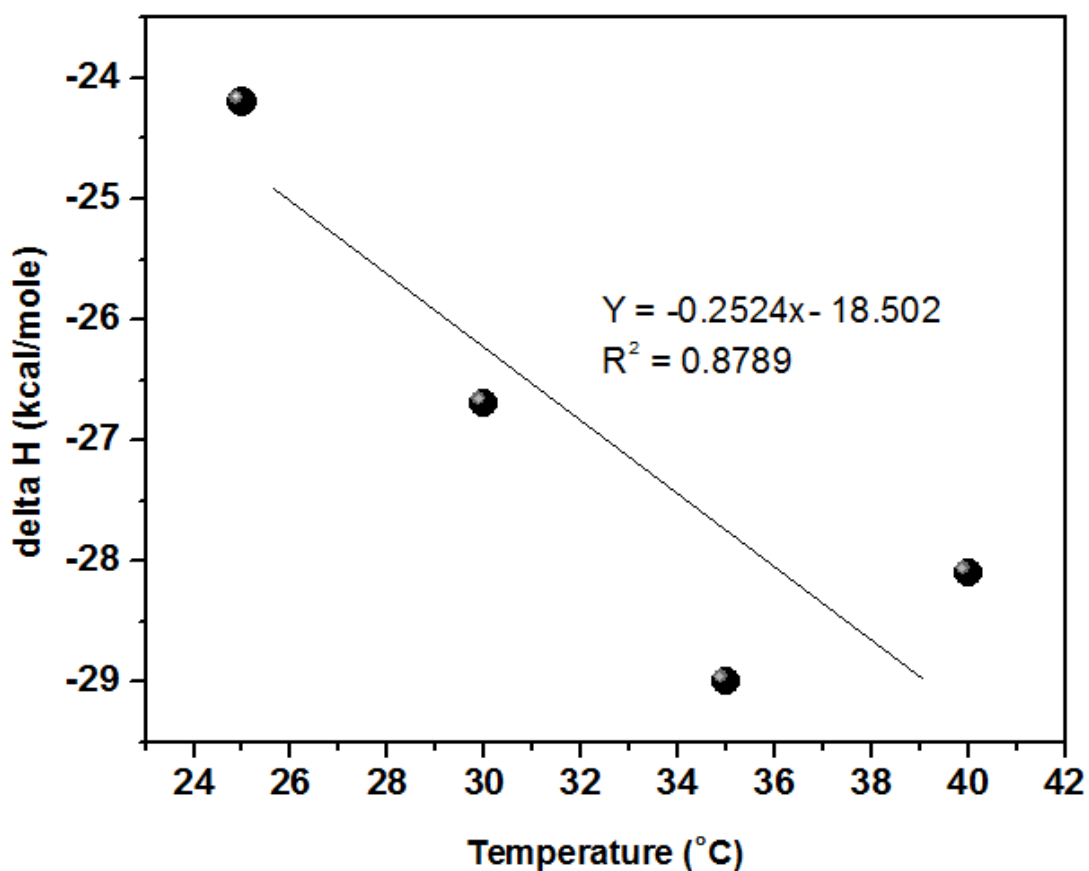


Figure 27. Determination of the change in heat capacity by the graph of ΔH as a function of temperature. The slope of the graph represents ΔC_p (in kcal/ mol °C).

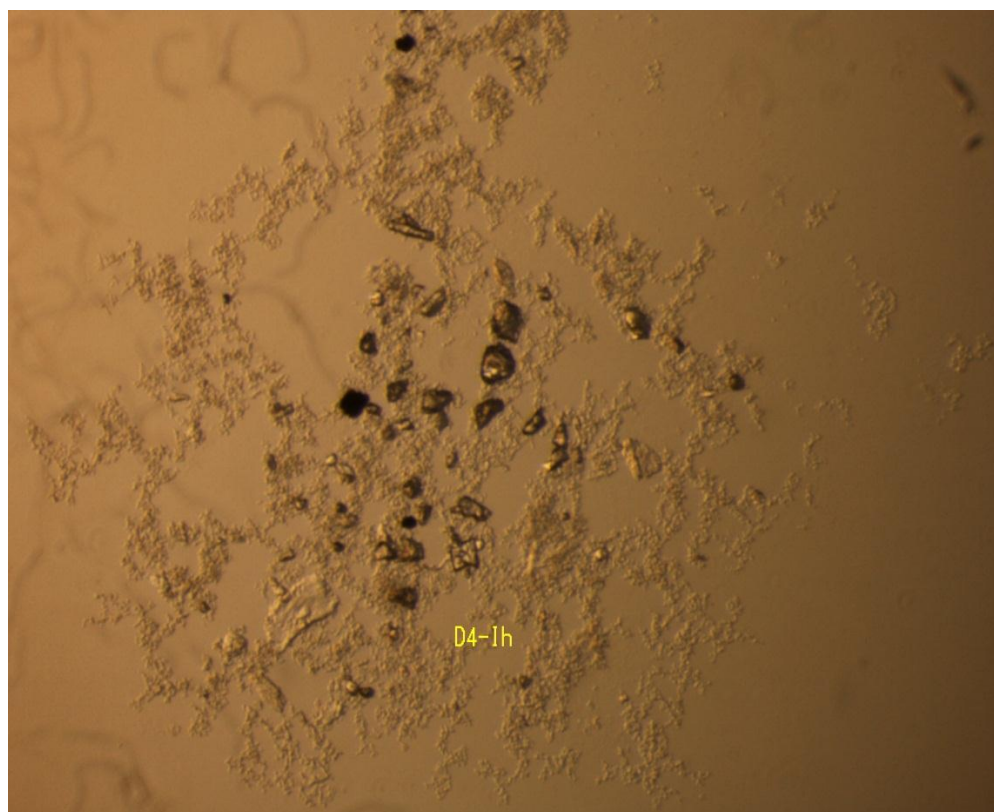


Figure 28. Optimization micro crystals of *Hscen1-HsSfi1*_{p21} complex. The precipitant solution used was 50% (v/v) 2-methyl-2,4-pentanediol (MPD) in 0.1 M Tris pH 8.5

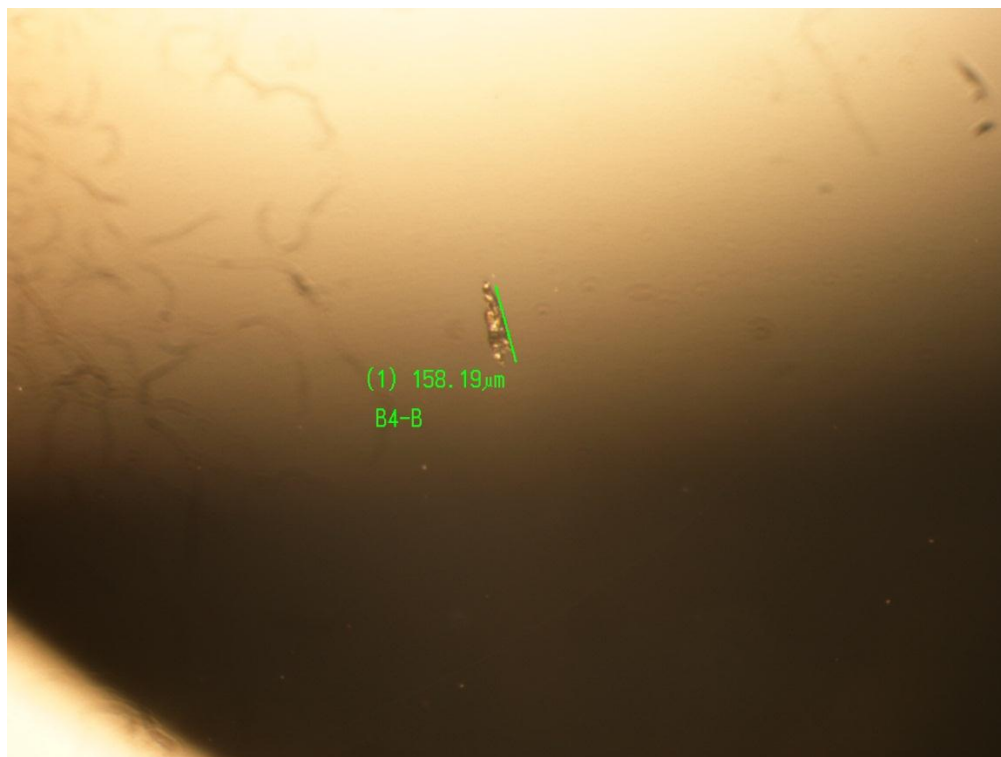


Figure 29. Optimization of needle crystals of *Hscen1-HsSfi1p₂₁* complex. The precipitant solution used was 50% (v/v) MPD in 0.1 M sodium acetate.



Figure 30. Optimization of crystals of *Hscen1-HsSfi1p₂₁* complex. The precipitant solution was 40% v/v 2-propanol.

A comparative analysis of the interaction between human centrin isoforms and HsSfi1p₂₁

In order to carry out a comparative analysis of the interaction between *Hscen1*, *Hscen2*, and *Hscen3* with *HsSfi1p₂₁*, ITC experiments were performed at 30°C to obtain the thermodynamic parameters of these interactions (Figure 31-32). As in the case of *Hscen1* (Figure 24), the interactions between *Hscen2* and *Hscen3* with *HsSfi1p₂₁* were exothermic. The ITC data of these two experiments were best fitted in the single-site binding model. Also, the stoichiometry of these complexes was 1:1. Table 2 presents the thermodynamic parameters of these complexes. *Hscen3-HsSfi1p₂₁* complex presents the most stable interaction ($\Delta G = -10.7$ kcal/mol) (Figure 33). Also, this complex corresponds to the highest affinity ($K_a = 5.1 \times 10^7 M^{-1}$). *Hscen1-HsSfi1p₂₁* complex has a more favorable enthalpy ($\Delta H = -26.7$ kcal/mol) and an unfavorable entropy ($-T\Delta S = 16.7$ kcal/mol). *Hscen2-HsSfi1p₂₁* complex had the lower affinity constant ($K_a = 0.9 \times 10^7 M^{-1}$). Analysis of the thermal stability of centrins carried out by Pastrana's group by differential scanning calorimetry (DSC), CD, and FTIR experiments performed in the temperature range of 10- 130°C suggest that *Hscen3* is the most stable isoform of human centrin. Together, these results revealed that the stability of the interaction between centrin and Sfi1p is dependent on the relative stability of centrin. Moreover, these results show that each centrin isoform binds *HsSfi1p₂₁* with a different affinity. Finally, these results may be applied towards the

understanding of centrin-Sfi1 interactions in general and the potential for phenotype rescue by using a different isoform of centrin.

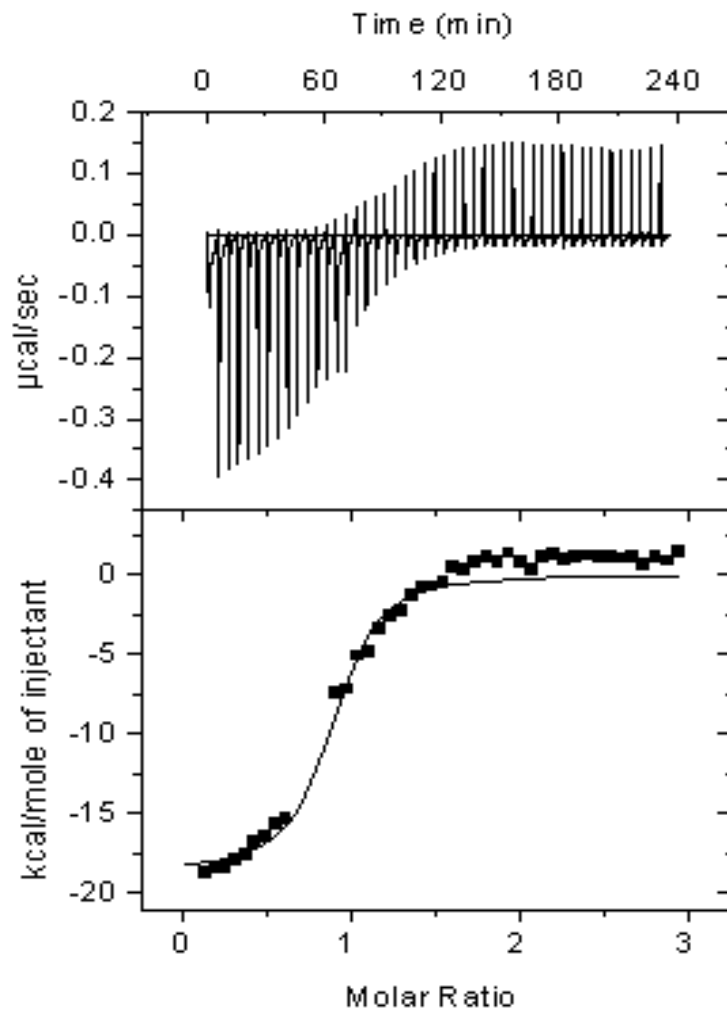


Figure 31. ITC isotherms of the interaction between *Hscen2* (WT) with *HsSfi1p₂₁* at 30°C. The upper panels show the raw data and the lower panels show the integrated enthalpy fitted to a single site-binding model.

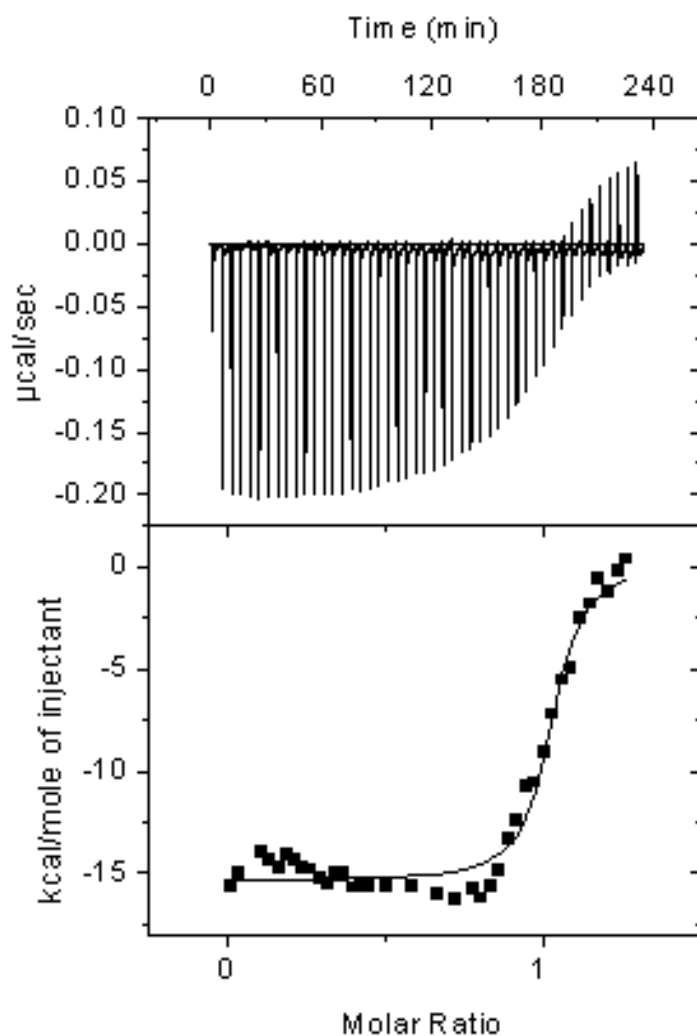


Figure 32. . ITC isotherms of the interaction between *Hscen3* (WT) with *HsSfi1p₂₁* at 30°C. The upper panels show the raw data and the lower panels show the integrated enthalpy fitted to a single site-binding model.

Table 4. Summary of the thermodynamic data of the interaction between *Homo sapiens* centrin isoforms with *HsSfi1p₂₁* at 30°C. The stoichiometry of binding is always close to 1.

Protein	Peptide	K _a (10 ⁷ M ⁻¹)	ΔG (kcal/mol)	ΔH (kcal/mol)	-TΔS (kcal/mol)
<i>Hscen1</i> (WT)	<i>HsSfi1p₂₁</i>	1.6 (0.2)	-10.0	-26.7 (0.2)	16.7
<i>Hscen2</i> (WT)	<i>HsSfi1p₂₁</i>	0.9 (0.2)	-9.6	-18.2 (0.5)	8.5
<i>Hscen3</i> (WT)	<i>HsSfi1p₂₁</i>	5.1 (0.8)	-10.7	-15.8 (0.1)	5.1

Note: The ITC profile was rendered the best fit when the Chi-squared (Chi²) value obtained 10⁵.

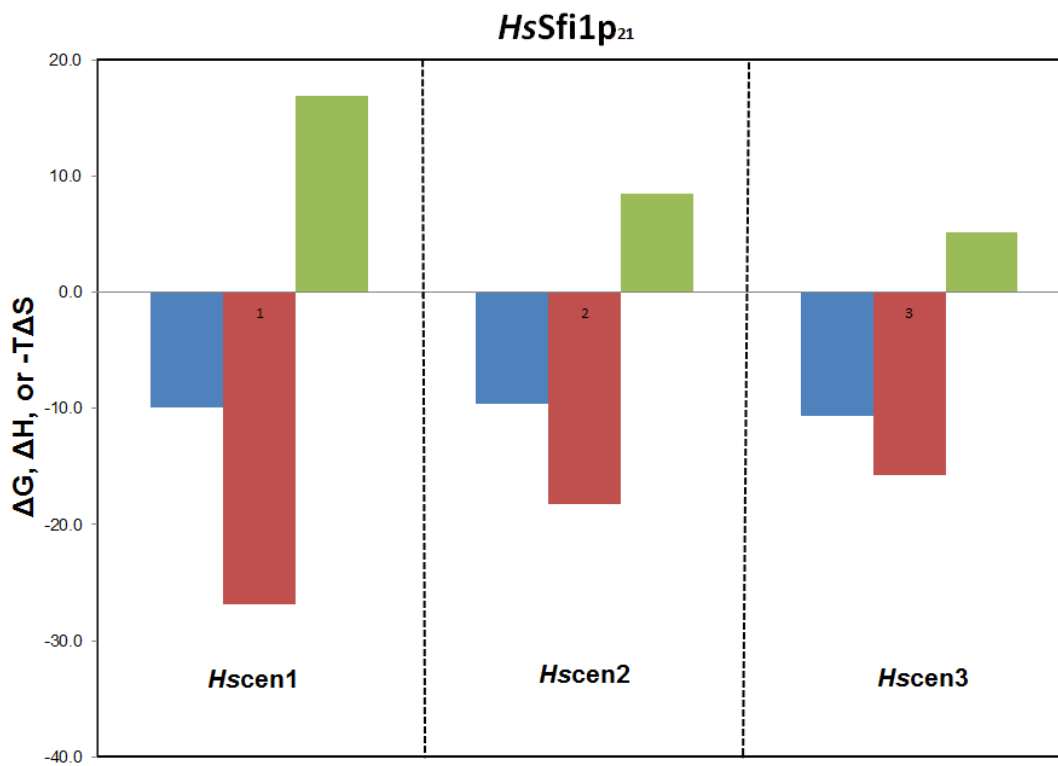


Figure 33. A comparative thermodynamic analysis of the interactions of *Homo sapiens* centrins and *HsSfi1p₂₁*. Comparison of the enthalpic (ΔH , red bar) and entropic ($-T\Delta S$, green bar) contributions to Gibbs free energy (ΔG , blue bar) of the interaction of *HsSfi1p₂₁* with *Hscen1*, *Hscen2*, and *Hscen3*, respectively. The experiments were carried out at 30°C and pH 7.4.

CHAPTER V

CONCLUSIONS

In this research, isothermal titration calorimetry was presented as a powerful tool to carry out thermodynamics studies of protein-protein interactions between *Homo sapiens* centrins and Sfi1p. By this technique, the thermodynamics governing binding of the full length centrin-Sfi1p₂₁ complex was determined. The interaction between *Hscen1* and *HsSfi1* is favored at 35°C which is near body temperature. The negative ΔC_p could be explained as a result of a decrease in exposure of hydrophobic surface as a result of the interaction between *Hscen1* and *HsSfi1*₂₁. These results support the fact that the hydrophobic triad located in the C-terminal end of *HsSfi1*₂₁ which is present in many of the centrin biological targets is essential for the interaction with a hydrophobic surface located in the C-terminal domain of centrin. By binding with calcium, centrin undergoes conformational changes that exposed this hydrophobic surface and allows the interaction with Sfi1p. As a result of the hydrophobic interactions that occur between centrin and Sfi1p, the hydrophobic surface area that is located in the interface decreased, and hence, a negative change in heat capacity was observed.

The results of the comparative analysis of the interaction of the human centrins with *HsSfi1*₂₁ show that the stability of the interaction between centrin

and Sfi1p is affected by the relative stability of centrin. Because human centrin 3 is the most stable centrin isoform, its interaction with *HsSfi1p₂₁* presents the highest stability and affinity, followed by *Hscen1-HsSfi1p₂₁* and *Hscen2-HsSfi1p₂₁* complexes, respectively.

CHAPTER VI

FUTURE WORK

The crystals obtained in this research will be analyzed by X-Ray diffraction to obtain its diffraction pattern to allow for the determination of a novel *Hscen1-HsSfi1p₂₁* complex structure and determine the numbers of calcium binding sites that are required for complex interaction. Also, the structure of the centrin-Sfi1p₂₁ complex should be determined and analyze and the hydrophobic interactions that are observed should be analyzed. Further investigation of the interaction between mutant centrins with Sfi1p by ITC will be useful in order to determine the amino acids that affect significantly the binding of centrin with Sfi1p. Also, it will very helpful to carry out ITC experiments of *Hscen2* and *Hscen3* with *HsSfi1p₂₁* at different temperatures in order to determine the ΔC_p of the binding and compare these results with the ΔC_p of the *Hscen1-HsSfi1p₂₁* obtained in this research thesis. Azimzadeh et al. in 2009 [63] show that POC5 is a biological target of centrin. This protein has Sfi1p-like centrin binding sites, thus, it will be useful to perform thermodynamic studies of the interaction between centrin and POC5 by ITC in order compare the affinity and stability of the interactions between Sfi1p and POC5p with centrin.

REFERENCES

1. Kilmartin, J.V. (2003) Sfi1p has conserved centrin-binding sites and an essential function in budding yeast spindle body duplication. *J. Cell. Biol.* 162, 1211-1221.
2. Salisbury, J.L. (2004) Centrosomes: Sfi1p and centrin unravel a structural riddle. *Curr. Biol.* 14, 27-29.
3. Salisbury, J.L. (2007) A mechanistic view on the evolutionary origin for centrin-based control of centriole duplication. *J. Cell. Physiol.* 213, 420-428.
4. Martinez-Sanz, J., Yang, A., Blouquit, Y., Duchambon, P., Assairi, L., and Craescu, C.T. (2006) Binding of human centrin 2 to the centrosomal protein hSfi1. *FEBS J.* 273, 4504-4515.
5. Martines-Sanz, J., Kateb, F., Assairi, L., Blouquit, Y., Bondenhausen, G., Abergel, D., Mouawad, L., and Craescu, C.T. (2010) Structure, Dynamics and Thermodynamics of the Human Centrin 2/hSfi1 complex. *J. Mol. Biol.* 395, 191-204.
6. Leavitt, S., and Freire, E. (2001) Direct measurement of protein binding energetics by isothermal titration calorimetry. *Curr. Opin. Struct. Biol.* 11, 560-566.

7. Hu, H., and Chazin, W.J. (2003) Unique features in the C-terminal domain provide caltractin with target specificity. *J. Mol. Biol.* 330, 473-484.
8. Durussel, I., Blouquit, Y., Middendorp, S., Craescu, C.T., and Cox, J.A. (2000) Cation- and peptide binding properties of human centrin 2. *FEBS Lett.* 472, 208-212.
9. Yang, A., Miron, S., Mouawad, L., Duchambon, P., Blouquit, Y., and Craescu C.T. (2006) Flexibility and plasticity of human centrin 2 binding to the xeroderma pigmentosum group C protein (XPC) from nuclear excision repair. *Biochemistry.* 45, 3653-3663.
10. Salisbury, J.L., Baron, A., Surek, B., and Melkonian, M. (1984) Striated flagellar roots: isolation and partial characterization of a calcium-modulated contractile organelle. *J. Cell Biol.* 99, 962-970.
11. Hartman, H., and Federov, A. (2002) The origin of the eukaryotic cell: A genomic investigation. *Proc. Natl. Acad. Sci. USA* 99, 1420-1425.
12. Levy, Y.Y., Lai, E., Remillard, S.P., Heintzelman, M.B., and Fulton, C. (1996) Centrin is a conserved protein that forms diverse associations with centrioles and MTOC's in *Naegleria* and other organisms. *Cell Motil. Cytoskel.* 33, 298-323.
13. Klotz, C., De Loubresse, N.G., Ruiz, F., and Beisson, J. (1997) Genetic evidence for a role of centrin-associated proteins in the organization and dynamics of the infraciliary lattice in *Paramecium*. *Cell Motil. Cytoskel.* 38, 172-186.

14. Trojan, P., Krauss, N., Choe, H-W., Giebl, A., Pulvermüller, A., and Wolfrum, U. (2008) Centrioles in retinal photoreceptor cells: Regulators in the connecting cilium. *Progr. Ret. Eye Research*. 27, 237-259.
15. Giebl, A., Trojan, P., Pulvermüller, A., and Wolfrum, U. (2004) Centrioles, potential regulators of transducing translocation in photoreceptor cells. Williams DS (ed.) In: *Cell biology and related disease of the outer retina*. World Scientific. pp. 195-222.
16. Taillon, B.E., Adler, S.A., Suhan, J.P., and Jarvik, J.W. (1992) Mutational analysis of centriolin: an EF-hand protein associated with three distinct contractile fibers in the basal body apparatus of *Chlamydomonas*. *J. Cell Biol.* 119, 1613-1624.
17. Sanders, M.A., and Salisbury, J.L. (1994) Centriolin plays an essential role in microtubule severing during flagellar excision in *Chlamydomonas reinhardtii*. *J. Cell Biol.* 124, 795-805.
18. Dantas, T.J., Wang, Y., Lalor, P., Dockery, P., and Morrison, C.G. (2011) Defective nucleotide excision repair with normal centrosome structures and functions in the absence of all vertebrate centrioles. *J. Cell Biol.* 193, 307-318.
19. Middendorp, S., Paoletti, A., Schiebel, E., and Bornens, M. (1997) Identification of a new mammalian centriolin gene, more closely related to *Saccharomyces cerevisiae* CDC31 gene. *Proc. Natl. Acad. Sci. USA* 94, 9141-9146.

20. Hart, P.E., Glantz, J.N., Orth, J.D., Poynter, G.M., and Salisbury, J.L. (1999) Testis-specific murine centrin, Cen1: genomic characterization and evidence for retroposition of a gene encoding a centrosome protein. *Genomics*. 60, 111-120.
21. Palermo, G.D., Joris, H., Devroey, P., and Van Steirteghem, A.C. (1992) Pregnancies after intra cytoplasmic sperm injection of single spermatozoon into an oocyte. *Lancet*. 340, 17-18.
22. Sun, X., Ma, J., Ge, Y., Li, S., Yu, Z., Xue, S., and Han, D. (2002) Abnormal expression of centrosome protein (centrin) in spermatozoa of male human infertility. *Chinese Science Bulletin*. 47, 822-823.
23. Hinduja, I., Baliga, N.B., and Zaverik, K. (2010) Correlation of human sperm centrosomal proteins with fertility. *J. Hum. Reprod. Sci.* 3, 95-101.
24. Nakamura, S., Terada, Y., Rawe, V.Y., Uehara, S., Morito, Y., Yoshimoto, T., Tachibana, M., Murakami, T., Yaegashi, N., and Okamura, K. (2005) A trial to restore defective human sperm centrosomal function. *Hum. Reprod.* 20, 1933-1937.
25. Salisbury, J.L., Suino, K.M., Busby, R., and Springett, M. (2002) Centrin-2 is required for centriole duplication in mammalian. *Curr. Biol.* 12, 1287-1292.
26. Geimer, S., and Melkonian, M. (2005) Centrin scaffold in *Chlamydomonas reinhardtii* revealed by immunoelectron microscopy. *Eukar. Cell.* 4, 1253-1263.

27. Nishi, R., Okuda, Y., Watanabe, E., Mori, T., Iwai, S., Masutani, C., Sugasawa, K., and Hanaoka, F. (2005) Centrin 2 stimulates nucleotide excision repair by interacting with xeroderma pigmentosum group C protein. *Mol. Cell Biol.* 25, 5664-5674.
28. Araki, M., Masutani, C., Takemura, M., Uchida, A., Sugasawa, K., Kondoh, J., Ohkuma, Y., and Hanaoka, F. (2001) Centrosome protein centrin 2/caltractin 1 is part of the xeroderma pigmentosum group C complex that initiates global genome nucleotide excision repair. *J. Biol. Chem.* 276, 18665-18672.
29. Klein, U.R., and Nigg, E.A. (2009) SUMO-dependent regulation of centrin-2. *J. Cell Sci.* 122, 3312-3321.
30. Resendes, K.K., Rasala, B.A., and Forbes, D.J. (2008) Centrin 2 localizes to the vertebrate nuclear pore and plays a role in mRNA and protein export. *Mol. Cell Biol.* 28, 1755-1769.
31. Middendorp, S., Küntzinger, T., Abraham, Y., Holmes, S., Bordes, N., Paintrand, M., Paoletti, A., and Bornens, M. (2000) A role for centrin 3 in centrosome reproduction. *J. Cell Biol.* 148, 405-415.
32. Gavet, O., Alvarez, C., Gaspar, P., and Bornens, M. (2003) Centrin4p, a novel mammalian centrin specifically expressed in ciliated cells. *Mol. Biol. Cell.* 14, 1818-1834.

33. Gifford, J.L., Walsh, M.P., and Vogel, H.J. (2007) Structures and metal-ion-binding properties of the Ca⁺²-binding helix-loop-helix EF-hand motifs. *Biochem. J.* 405, 199-221.
34. Lewit-Bentley, A., and Réty S. (2000) EF-hand calcium-binding proteins. *Curr. Op. Struct. Biol.* 10, 637-643.
35. Kretsinger, R.H., and Nockolds C.E. (1973) Carp muscle calcium-binding protein. *J. Biol. Chem.* 248, 3313-3326.
36. Matei, E., Miron, S., Blouquit, Y., Duchambon, P., Durussel, I., Cox, J.A., and Craescu, C.T. (2003) C-terminal half of human centrin 2 behaves like a regulatory EF-hand domain. *Biochemistry.* 42, 1439-1450.
37. Sosa, L del V., Alfaro, E., Santiago, J., Narváez, D., Rosado, M.C., Rodríguez, A., Gómez, A.M., Schreiter, E.R., and Pastrana-Rios, B. (2011) The structure, molecular dynamics and energetics of centrin-melittin complex. *Proteins.* 79, 3132-3143.
38. Sheehan, J.H., Bunick, C.G., Hu, H., Fagan, P.A., Meyn, S.M., and Chazin, W.J. (2006) Structure of the N-terminal calcium sensor domain of centrin reveals the biochemical basis for domain-specific function. *J. Biol. Chem.* 281, 2876-2881.
39. Milos, M., Schaer, J-J., Compte, M., and Cox, J.A. (1987) Microcalorimetric investigation of the interactions in the ternary complex calmodulin-calcium-melittin. *J. Biol. Chem.* 262, 2746-2749.

40. Cox, J.A., Compte, M., Fitton, J.E., and DeGrado, W.F. (1985) The interaction of calmodulin with amphiphilic peptides. *J.Biol.Chem.* 260, 2527-2534.
41. Kataoka, M., Head, J.F., Seaton, B.A., and Engelman, D.M. (1989) Melittin binding causes a large calcium-dependent conformational change in calmodulin. *Proc. Natl. Acad. Sci. USA.* 86, 6944-6948.
42. Maulet, Y, and Cox, J.A. (1983) Structural changes in melittin and calmodulin upon complex formation and their modulation by calcium. *Biochemistry.* 22, 5680-5686.
43. Newman, R.A., Van Scyoc, W.S., Sorensen, B.R., Jaren, O.R., and Shea, M.A. (2008) Interdomain cooperativity of calmodulin bound to melittin preferentially increases calcium affinity of sites I and II. *Proteins.* 71, 1792-1812.
44. Cox, J.A., Tirone, F., Durussel, I., Firanescu, C., Blouquit, Y., Duchambon, P., and Craescu, C.T. (2005) Calcium and magnesium binding of human centrin 3 and interaction with target peptides. *Biochemistry.* 44, 840-850.
45. Thompson, J.R., Ryan, Z.C., Salisbury, J.L., and Kumar, R. (2006) The structure of the human centrin 2 - xeroderma pigmentosum group C protein complex. *J. Biol. Chem.* 281, 18746-18752.
46. Biggins, S., and Rose, M.D. (1994) Direct interaction between yeast spindle pole body components: Kar1p is required for Cdc31p localization to the spindle pole body. *J. Cell. Biol.* 125, 843-852.

47. Spang, A., Courtney, I., Grein, K., Matzner, M., and Schiebel, E. (1995) The Cdc31p-binding protein Kar1p is a component of the half bridge of the yeast spindle pole body. *J. Cell Biol.* 128, 863-877.
48. Veeraraghavan, S., Fagan, P.A., Hu, H., Lee, V., Harper, J.F., Huang, B., and Chazin W.J. (2002) Structural independence of the two EF-hand domains of caltractin. *J. Biol. Chem.* 277, 28564-28571.
49. Hu, H., Sheehan, J.H., and Chazin, W.J. (2004) The mode action of centrin: Binding of Ca^{+2} and a peptide fragment of Kar1p to the C-terminal domain. *J. Biol. Chem.* 279, 50895-50903.
50. Miron, S., Durand, D., Chilom, C., Pérez, J., and Craescu, C.T. (2011) Binding of calcium, magnesium, and target peptides to Cdc31, the centrin of yeast *Saccharomyces cerevisiae*. *Biochemistry.* 50, 6409-6422.
51. Fischer, T., Rodríguez-Navarro, S., Pereira, G., Rácz, A., Schiebel, E., and Hurt, E. (2004) Yeast centrin Cdc31 is linked to the nuclear mRNA export machinery. *Nat. Cell Biol.* 6, 840-848.
52. Jani, D., Lutz, S., Marshall, N.J., Fischer, T., Köhler, A., Ellisdon, A.M., Hurt, E., and Murray, S. (2009) Sus1, Cdc31, and the Sac3 CID region form a conserved interaction platform that promotes nuclear pore association and mRNA export. *Mol. Cell.* 33, 727-737.
53. Ma, P., Winderickx, J., Nauwelaers, D., Dumortier, F., De Doncker, A., Thevelein, J.M., and Van Dijck, P. (1999) Deletion of SFI1, a novel

- suppressor of partial Ras-cAMP pathway deficiency in the yeast *Saccharomyces cerevisiae*, causes G₂ arrest. *Yeast*. 15, 1097-1109.
54. Li, S., Sandercock, A.M., Conduit, P., Robinson, C.V., Williams, R.L., and Kilmartin, J.V. (2006) Structural role of Sfi1p-centrin filaments in budding yeast spindle pole body duplication. *J. Cell Biol.* 173, 867-877.
 55. Pierce, M.M., Raman, C.S., and Nall, B.T. (1999) Isothermal titration calorimetry of protein-protein interactions. *Methods*. 19, 213-221.
 56. Serdyuk, I.N., Zaccai, N.R., and Zaccai, J. (2007) *Methods in molecular biophysics: Structure, dynamics, function*. Cambridge University Press, Cambridge, pp. 221-233.
 57. Wiseman, T., Willinston, S., Brandts, J.F., and Lin, L.N. (1989) Rapid measurement of binding constants and heats of binding using a new titration calorimeter. *Anal. Biochem.* 179, 131-137.
 58. Freire E. 2004. Isothermal titration calorimetry: controlling binding forces in lead optimization. *Drug Discovery Today: Technologies*. 1:295-299.
 59. Ross, P.D., and Subramanian, S. (1981) Thermodynamics of protein association reactions: forces contributing to stability. *Biochemistry*. 20, 3096-3102.
 60. Uedaira, H., Kono, H., Ponraj, P., Kitajima, K., and Sarai, A. (2003) Structure-thermodynamic relationship in protein-DNA binding: Heat capacity changes. *Genome Informatics*. 14, 510-511.

61. Pastrana-Rios, B., Ocaña, W., Rios, M., Vargas, G.L., Ysa, G., Poynter, G., Tapia, J., and Salisbury J.L. (2002) Centrin: Its secondary structure in the presence and absence of cations. *Biochemistry*. 41, 6911-6919.
62. <http://cti.itc.virginia.edu/~cmg/Demo/wheel/wheelApp.html>. (Accessed on April 2012).
63. Azimzadeh, J., Hergert, P., Delouvé, A., Euteneuer, U., Formstecher, E., Khodjakov, and Bornens, M. (2009) hPOC5 is a centrin-binding protein required for assembly of full-length centrioles. *J. Cell Biol.* 185, 101-114.

APPENDIX A

Publications

- Pastrana-Rios, B., De Orbeta, J., Meza, V., Reyes, M., Narváez, D., Gómez, A.M., Rodríguez-Nassif, A., Almodovar, R., Díaz-Casas, A., Robles, J., Ortiz, A.M., Irizarry, L., Campbell, M., and Colón M. (2012) Relative stability of human centrin's and its relationship with their calcium binding sites. *Submitted to Biochemistry.*

Presentations

- Poster Presentation. 2012 Lilly Academy Technical Forum. San Juan, Puerto Rico. April 13, 2012.
- Poster Presentation. IFPAC/PAT Summer Summit. San Juan, Puerto Rico. June 12-13, 2012.

APPENDIX B

Table. Summary of centrin-biological target complexes cited in this thesis.

Protein	Peptide	Reference
Cdc31 (full length)	Sc Sfi1 (N ₂₁₈ -H ₃₀₆)	Li et al. 2006 [1]
Hscen2 (T ₉₄ -Y ₁₇₂)	Hs Sfi1 (R ₆₄₁ -T ₆₆₀)	Martinez-Sanz et al. 2006 [4-5]
Crcen (G ₉₃ -F ₁₆₉)	Kar1 (K ₂₃₉ -K ₂₅₇)	Hu et al. 2003 [7]
Hs cen2 (full-length)	MLT (full length)	Durussel et al. 2000 [8]
Crcen (full length)	MLT (full length)	Sosa et al. 2011 [37]
Hs cen3 (E ₂₁ -D ₁₁₂)	MLT (full length)	Cox et al. 2005 [44]
Hscen2 (full length)	Hs XPC (N ₈₄₇ -R ₈₆₃)	Thompson et al. 2006 [45]
Cdc31 (full length)	ScSac3 (E ₇₅₃ -S ₈₀₅)	Jani et al. 2009 [52]
Cdc31 (full length)	ScSac3 (K ₇₉₇ -I ₈₁₄)	Miron et al. 2011 [50]

APPENDIX C

Scheme. Sequence alignment of the 23 tandem centrin binding sites of *Homo sapiens* Sfi1. The positions marked in green represents conserved positions constitute primarily with hydrophobic residues in the CBS.

	1	10	20	30	33																												
<i>HsSfi1p</i> ₁ (103-135)	T	F	G	R	V	F	P	S	K	A	R	F	Y	Y	E	Q	R	L	L	R	K	V	F	E	E	W	K	E	E	W	W	V	F
<i>HsSfi1p</i> ₂ (136-168)	Q	H	E	W	K	L	C	V	R	A	D	C	H	Y	R	Y	Y	L	Y	N	L	M	F	Q	T	W	K	T	Y	V	R	Q	Q
<i>HsSfi1p</i> ₃ (169-201)	Q	E	M	R	N	K	Y	I	R	A	E	V	H	D	A	K	Q	K	M	R	Q	A	W	K	S	W	L	I	Y	V	V	R	
<i>HsSfi1p</i> ₄ (202-234)	R	T	K	L	Q	M	Q	T	T	A	L	E	F	R	Q	R	I	I	L	R	V	W	W	S	T	W	R	Q	R	L	G	Q	V
<i>HsSfi1p</i> ₅ (225-267)	R	V	S	R	A	L	H	A	S	A	L	K	H	R	A	L	S	L	Q	V	Q	A	W	S	Q	W	R	E	Q	L	L	Y	V
<i>HsSfi1p</i> ₆ (268-300)	Q	K	E	K	Q	K	V	V	S	A	V	K	H	H	Q	H	W	Q	K	R	R	F	L	K	A	W	L	E	Y	L	Q	V	R
<i>HsSfi1p</i> ₇ (301-333)	R	V	K	R	Q	Q	N	E	M	A	E	R	F	H	H	V	T	V	L	Q	I	Y	F	C	D	W	Q	Q	A	W	E	R	R
<i>HsSfi1p</i> ₈ (334-366)	E	S	L	Y	A	H	H	A	Q	V	E	K	L	A	R	K	M	A	L	R	R	A	F	T	H	W	K	H	Y	M	L	L	C
<i>HsSfi1p</i> ₉ (367-399)	A	E	E	A	A	Q	F	E	M	A	E	E	H	H	R	H	S	Q	L	Y	F	C	F	R	A	L	K	D	N	V	T	H	A
<i>HsSfi1p</i> ₁₀ (400-432)	H	L	Q	Q	I	R	R	N	L	A	H	Q	Q	H	G	V	T	L	L	H	R	F	W	N	L	W	R	S	Q	I	E	Q	K
<i>HsSfi1p</i> ₁₁ (434-467)	E	R	E	L	L	P	L	H	A	A	W	D	H	Y	R	I	A	L	L	C	K	C	I	E	L	W	L	Q	Y	T	Q	K	R
<i>HsSfi1p</i> ₁₂ (468-500)	R	Y	K	Q	L	L	Q	A	R	A	D	G	H	F	Q	Q	R	A	L	P	A	A	F	H	T	W	N	R	L	W	R	W	R
<i>HsSfi1p</i> ₁₃ (501-533)	H	Q	E	N	V	L	S	A	R	A	T	R	F	H	R	E	T	L	E	K	Q	V	F	S	L	W	R	Q	K	M	F	Q	H
<i>HsSfi1p</i> ₁₄ (534-566)	R	E	N	R	L	A	E	R	M	A	I	L	H	A	E	R	Q	L	L	Y	R	S	W	F	M	W	H	Q	Q	A	A	A	R
<i>HsSfi1p</i> ₁₅ (567-599)	H	Q	E	Q	E	W	Q	T	V	A	C	A	H	H	R	H	G	R	L	K	K	A	F	C	L	W	R	E	S	A	Q	G	L
<i>HsSfi1p</i> ₁₆ (600-632)	R	T	E	R	T	G	R	V	R	A	E	F	H	M	A	Q	L	L	R	W	A	W	S	Q	W	R	E	C	L	A	L	R	
<i>HsSfi1p</i> ₁₇ (633-665)	G	A	E	R	Q	K	L	M	R	A	D	L	H	H	Q	H	S	V	L	H	R	A	L	Q	A	W	V	T	Y	Q	G	R	V
<i>HsSfi1p</i> ₁₈ (666-698)	R	S	I	L	R	E	V	A	A	R	E	S	Q	H	N	R	Q	L	L	R	G	A	L	R	R	W	K	E	N	T	M	A	R
<i>HsSfi1p</i> ₁₉ (699-731)	V	D	E	A	K	K	T	F	Q	A	S	T	H	Y	R	R	T	I	C	S	K	V	L	V	Q	W	R	E	A	V	S	V	Q
<i>HsSfi1p</i> ₂₀ (736-768)	Q	Q	E	D	C	A	I	W	E	A	Q	K	V	L	D	R	G	C	L	R	T	W	F	Q	R	W	W	D	C	S	R	R	S
<i>HsSfi1p</i> ₂₁ (769-801)	A	Q	Q	R	L	Q	L	E	R	A	V	Q	H	H	H	R	Q	L	L	L	E	G	L	A	R	W	K	T	H	H	L	Q	C
<i>HsSfi1p</i> ₂₂ (802-834)	V	R	K	R	L	L	H	R	Q	S	T	Q	L	L	A	Q	R	L	S	R	T	C	F	R	Q	W	R	Q	Q	L	A	A	R
<i>HsSfi1p</i> ₂₃ (835-867)	R	Q	E	Q	R	A	T	V	R	A	L	W	F	W	A	F	S	L	Q	A	K	V	W	A	T	W	W	F	S	L	Q	A	K